The catalytic function of the gephyrin-binding protein IQSEC3 regulates neurotransmitter-specific matching of pre- and post-synaptic structures in primary hippocampal cultures

Früh, Simon ; Tyagarajan, Shiva K ; Campbell, Benjamin ; Bosshard, Giovanna ; Fritschy, Jean-Marc

Abstract: In dissociated neuronal cultures the absence of spatial and temporal cues causes the emergence of mismatched synapses, where post-synaptic proteins of GABAergic synapses are in part apposed to glutamatergic pre-synaptic terminals and vice versa. This mismatch offers an opportunity to study the mechanisms that regulate correct apposition of pre- and post-synaptic elements. We report here that the IQ motif and Sec7 domain-containing protein 3 (IQSEC3; BRAG3; synArfGEF) specifically regulates the mislocalization of GABAergic post-synaptic density (PSD) proteins. Over-expression of IQSEC3 constructs harboring mutations that ablate Sec7 domain or IQ motif function revealed that IQSEC3 catalytic activity is involved in the control of apposition between the GABAergic PSD and glutamatergic terminals. Neurons co-expressing eGFP-gephyrin with IQSEC3 Sec7 mutant displayed a drastically increased fraction of mismatched eGFP-gephyrin clusters compared to other IQSEC3 constructs. Along with eGFP-gephyrin, endogenous GABA receptor cluster mismatching was increased by IQSEC3 Sec7 mutant over-expression. Conversely, GFP-PSD-95 clusters were unaffected by over-expression of any IQSEC3 construct. The GABAergic PSD mismatch phenotype was recapitulated by Arf6 dominant-negative mutant over-expression, suggesting that Arf6 activation by IQSEC3 is an essential step in this pathway. In addition, we provide biochemical evidence to confirm gephyrin/IQSEC3 interaction near the IQSEC3 IQ motif, which in turn binds calmodulin at low Ca concentrations. Taken together, our findings identify a post-synaptic protein which specifically regulates correct apposition of the GABAergic PSD to pre-synaptic terminals.

DOI: https://doi.org/10.1111/jnc.14572

The catalytic function of the gephyrin-binding protein IQSEC3 regulates neurotransmitter-specific matching of pre- and postsynaptic structures in primary hippocampal cultures

Simon Früh[1,2], Shiva K. Tyagarajan[1,2], Benjamin Campbell[1,2], Giovanna Bosshard[1], Jean-Marc Fritschy[1,2]

[1]Institute of Pharmacology and Toxicology, University of Zurich, 8057 Zurich, Switzerland

[2]Neuroscience Center Zurich, University of Zurich and Federal Institute of Technology (ETH) Zurich, 8057 Zurich, Switzerland

Corresponding author: Jean-Marc Fritschy, Institute of Pharmacology and Toxicology, Winterthurerstrasse 190, 8057 Zurich, Switzerland, Tel. +41 44 635 59 26, fritschy@pharma.uzh.ch

Running title: IQSEC3 regulates synaptic apposition

Keywords: SynArfGEF, Arf6, postsynaptic density, gephyrin, GABA, synapse formation

List of abbreviations: AA, amino acid; Arf, ADP-ribosylation factor; CNS, central nervous system; CA, constitutively active; DN, dominant negative; DMEM, Dulbecco's Modified Eagle Medium; FCS, fetal calf serum; $GABA_AR$, $GABA_A$ receptor; GEF, guanine nucleotide exchange factor; NL, neuroligin; NGS, normal goat serum; PSD, postsynaptic density; PBS, phosphate-buffered saline; PEI, polyethylenimine; RT, room temperature; TBST, Tris-buffered saline with 0.05% Tween 20.

Abstract

In dissociated neuronal cultures the absence of spatial and temporal cues causes the emergence of mismatched synapses, where postsynaptic proteins of GABAergic synapses are in part apposed to glutamatergic presynaptic terminals and vice versa. This mismatch offers an opportunity to study the mechanisms that regulate correct apposition of pre- and postsynaptic elements. We report here that the IQ motif and Sec7 domain-containing protein 3 (IQSEC3; BRAG3; synArfGEF) specifically regulates the mislocalization of GABAergic postsynaptic density (PSD) proteins. Overexpression of IQSEC3 constructs harboring mutations that ablate Sec7 domain or IQ motif function revealed that IQSEC3 catalytic activity is involved in the control of apposition between the GABAergic PSD and glutamatergic terminals. Neurons co-expressing eGFP-gephyrin with IQSEC3 Sec7 mutant displayed a drastically increased fraction of mismatched eGFP-gephyrin clusters compared to other IQSEC3 constructs. Along with eGFP-gephyrin, endogenous $GABA_A$ receptor cluster mismatching was increased by IQSEC3 Sec7 mutant overexpression. Conversely, GFP-PSD-95 clusters were unaffected by overexpression of any IQSEC3 construct. The GABAergic PSD mismatch phenotype was recapitulated by Arf6 dominant-negative mutant overexpression, suggesting that Arf6 activation by IQSEC3 is an essential step in this pathway. In addition, we provide biochemical evidence to confirm gephyrin/IQSEC3 interaction near the IQSEC3 IQ motif, which in turn binds calmodulin at low Ca^{2+} concentrations. Taken together, our findings identify a postsynaptic protein which specifically regulates correct apposition of the GABAergic PSD to presynaptic terminals.

Introduction

Alignment of presynaptic terminals of each neurotransmitter with postsynaptic densities (PSD) containing the corresponding postsynaptic receptors along with scaffolding and effector proteins is a fundamental requirement for neurotransmission at chemical synapses. Most neurons in the mammalian central nervous system (CNS) are innervated by axon terminals with a wide range of neurochemical compositions and synapses employing different neurotransmitter systems are often in close proximity. Yet, mismatched pre- and postsynaptic structures are virtually absent *in vivo*. Temporal differences in synapse formation between neurotransmitter systems do not fully account for correct apposition since synapse formation and elimination are life-long processes (Tyzio *et al.* 1999, Khazipov *et al.* 2001, Caroni *et al.* 2014). Molecular mechanisms must therefore contribute to the fidelity of apposition between neurotransmitter-specific pre- and postsynaptic elements.

Synapse formation is initiated by cell adhesion through homophilic trans-synaptic adhesion complexes, which are not neurotransmitter-specific (Missler *et al.* 2012). Differentiation of postsynaptic structures into specializations suited for a given neurotransmitter released from presynaptic terminals is achieved after initial contact formation by signaling molecules, of which only few are known to date. One of the best described mechanisms of neurotransmitter-specific induction of postsynaptic differentiation is dependent on alternative splicing of neurexin and neuroligin (NL). Isoform-specific splice inserts in NL extracellular domains interact with neurexins, promoting neurotransmitter-specific presynaptic differentiation . While other trans-synaptic molecules are known to be involved in promotion of neurotransmitter-specific differentiation, factors responsible for suppressing mismatched synaptic structures were not described thus far.

Although *in vivo* misalignment of pre- and postsynaptic structures is very rare (but see (Fritschy *et al.* 2006)), formation of mismatched synapses is common in dissociated neuronal cultures (Christie *et al.* 2002, Rao *et al.* 2000, Brunig *et al.* 2002). Both $GABA_A$ receptors ($GABA_AR$) and AMPA receptors are found in apposition to inappropriate axon terminals. Appearance of mismatched synapses in dissociated cultures is a consequence of the lack of

spatial and temporal cues that guide synapse formation *in vivo*. However, although the altered situation in dissociated neurons does not directly correspond to the situation *in vivo*, the presence of mismatched synapses in neuronal cultures provides an opportunity to study the molecular underlinings of synapse validation. The observation that the fraction of mismatched synapses in primary neurons is reduced with time in culture suggests that correction mechanisms ensure appropriate apposition after synapse formation. Since pharmacological activation of $GABA_A$ or NMDA receptors influences the abundance of mismatched synapses, such mechanisms are likely activity-dependent (Anderson *et al.* 2004).

IQ motif and Sec7 domain-containing protein 3 (IQSEC3; BRAG3; synArfGEF) is a guanine nucleotide exchange factor (GEF) for small GTPases of the ADP-ribosylation factor (Arf) family and is strongly expressed in the brain (Kikuno *et al.* 1999). The protein was first described as part of the glutamatergic PSD because of immunoreactivity in the PSD fraction and the presence of a C-terminal PDZ-domain binding motif (Inaba *et al.* 2004). Subsequent investigations concluded that IQSEC3 is principally located at GABAergic postsynaptic sites, on the basis of immunohistochemical analyses by light and electron microscopy and due to its binding to dystrophin (Fukaya *et al.* 2011, Sakagami *et al.* 2013). Like all Arf GEFs, IQSEC3 contains a catalytic Sec7 domain. The specificity of its GEF function is still unclear, since rat IQSEC3 showed activity for Arf6 but not Arf1 whereas the opposite was reported for the human homolog (Fukaya et al. 2011, Hattori *et al.* 2007). Interestingly, the close IQSEC3 homologs IQSEC1 and IQSEC2 are located in the glutamatergic PSD and regulate endocytosis of GluA2- and GluA1-containing AMPA receptors, respectively (Myers *et al.* 2012, Scholz *et al.* 2010). IQSEC3 functions at the synapse were not yet described but the nearly identical domain structure of IQSEC3 and its homologs suggests parallels in the role of IQSEC3 at the GABAergic PSD. Notably, all three homologs contain an IQ motif, which is known to bind calmodulin in a Ca^{2+}-dependent manner, and might thereby tie catalytic function to synaptic activity also in IQSEC3 (Bähler & Rhoads 2002).

Here, we explored the molecular mechanisms governing the correct alignment of pre- and postsynaptic structures in primary neuronal cultures. In particular, we addressed the question whether a postsynaptic protein like IQSEC3 is capable of regulating mismatched postsynaptic proteins and whether such regulation is neurotransmitter-specific. By taking an overexpression approach using various mutated and truncated forms of IQSEC3, we report that the catalytic function of IQSEC3 specifically controls misapposition between proteins of the GABAergic PSD and glutamatergic axon terminals. Similar alterations in mismatched synapses were found with overexpression of Arf6 mutants, suggesting that activation of Arf6 by IQSEC3 is an essential step in this pathway. Colocalization and biochemical interaction with gephyrin validated the proximity of IQSEC3 to GABAergic postsynaptic structures and the finding of Ca^{2+}-dependent calmodulin binding to IQSEC3 supported the notion that regulation of mismatched synapses is an activity-dependent process. Taken together, our experiments uncovered a neurotransmitter-specific process aimed at controlling formation of mismatched synapses in primary hippocampal cultures.

Materials and Methods

Constructs. pCIneo-FLAG-IQSEC3 plasmid was provided by Dr. Hiroyuki Sakagami and encodes FLAG-tagged rat IQSEC3 (NCBI NM_207617.1). The insert was PCR amplified and subcloned into the same vector using restriction sites EcoRI and NotI to avoid double insertion and remove part of IQSEC3 3'-UTR which was present in the original plasmid. Site-directed mutagenesis of the resulting plasmid was achieved through whole-plasmid amplification using point-mutated primers with Pfu Ultra Hotstart DNA Polymerase (Agilent, Santa Clara, CA). The E749K mutation was selected based on abolition of catalytic activity of IQSEC2 by a homologous mutation (E849K) (Myers et al. 2012), as well as in ARNO (E156K) (Cherfils *et al.* 1998, Mossessova *et al.* 1998). Template was digested with DpnI, DNA purified with GenElute PCR Clean-up kit (Merck, Darmstadt, Germany) and electrocompetent *E. coli* were transformed with purified mutated plasmids. Inserts were validated by control digestion and by sequencing. ΔPH deletion construct lacks the 111 amino acids (AA) of the PH domain and was created by whole-plasmid amplification with Pfu

Ultra Hotstart DNA polymerase using 5'-phosphorylated primers on either side of PH domain. Truncations were created by PCR amplification of IQSEC3 regions and subcloning into pCIneo-FLAG vector using restriction sites EcoRI and NotI. The following truncations were made: ΔN construct (AA183-1194); CC domain (AA1-182); IQ domain (AA183-650); IQ fragment 1 (AA183-335); IQ fragment 2 (AA336-499); IQ fragment 3 (AA500-650); Sec7 domain (AA651-840); PH / PP domain (AA841-1194). For mCherry-IQSEC3 fusion constructs, FLAG sequence was removed in pCIneo-FLAG-IQSEC3 constructs using restriction sites NheI and EcoRI and replaced by directional cloning of PCR-amplified mCherry containing restriction sites NheI at 5'-end and EcoRI at 3'-end.

Antibodies. Primary antibodies used in Western blots: Mouse anti-FLAG (1:5000; clone M2; Merck; RRID:AB_439685), rabbit anti-GFP (1:5000; Synaptic Systems, Göttingen, Germany; RRID:AB_10550537), rabbit anti-mCherry (1:1000; Abcam, Cambridge, UK; RRID:AB_2571870). Primary antibodies used for immunocytochemistry: Mouse anti-FLAG (1:5000; clone M2; Merck), rat anti-hemagglutinin (HA; 1:2000; clone 3F10; Roche; RRID:AB_2314622), mouse anti-gephyrin (1:1000; Synaptic Systems; RRID:AB_887719), guinea pig anti-$GABA_AR$ α2 subunit (1:5000; (Fritschy & Mohler 1995)), guinea pig anti-$GABA_AR$ γ2 subunit (1:5000; (Fritschy & Mohler 1995)), rabbit and guinea pig anti-IQSEC3 (both 1:1000; gift from Dr. Hiroyuki Sakagami (Fukaya et al. 2011)), rabbit anti-VGAT (1:3000; Synaptic Systems; RRID:AB_2315584), rabbit anti-VGluT1 (1:5000; Synaptic Systems; RRID:AB_887875), rabbit anti-VGluT2 (1:5000; Synaptic Systems; RRID:AB_887883). All antibodies are routinely used in the laboratory and have been extensively validated for use in Western blotting and immunocytochemistry.

HEK cell transfection. HEK293T cells (ATCC® CRL-3216™; RRID: CVCL_0063) were kept in Dulbecco's Modified Eagle Medium (DMEM; Thermo Fisher Scientific, Waltham, MA) containing 10% fetal calf serum (FCS) at 37 °C in 5% CO_2. Prior to transfection, HEK cells were passaged and grown to approximately 60% confluency. Medium was replaced with fresh DMEM containing 10% FCS 2 h before transfection. A total of 3 µg of DNA was mixed with polyethylenimine (PEI; 75 µg/mL) in 150 mM NaCl solution. After incubation at room

temperature (RT) for 30 min, the mix was added dropwise to HEK cells. HEK cells were kept in culture for 24 h before lysis.

Western blotting. HEK cells were rinsed carefully with ice-cold phosphate-buffered saline (PBS) and lysed in 50 mM Tris (pH 7.6), 120 mM NaCl, 0.5% NP-40 containing protease inhibitors (Complete Mini Protease Inhibitor Cocktail [Roche, Basel, Switzerland]) by shaking on a compensator for 20 min at 4 °C. Lysates were centrifuged at 20'000 RPM for 20 min at 4 °C and supernatants were stored at -80 °C. Samples were mixed with Laemmli buffer, boiled at 90 °C and run on tris-glycine polyacrylamide gels. Proteins were transferred to polyvinylidene fluoride membranes. Primary antibodies were incubated in Tris-buffered saline with 0.05% Tween 20 (TBST) including 5% Western Blocking Solution (Roche) ON at 4 °C. Membranes were washed 5 times in TBST. Horseradish peroxidase-coupled donkey secondary antibodies (1:20'000) were incubated for 1h at RT and membranes were washed again 5 times in TBST. SuperSignal West Pico Chemiluminescent Substrate (Thermo Fisher Scientific, Waltham, MA) was applied and membranes were developed on X-ray film (Fujifilm, Tokyo, Japan).

Immunoprecipitation. HEK cell lysates were incubated with 1 µg of immunoprecipitation antibody on a rotator for 3 h at 4 °C. Protein G-agarose beads in EBC buffer (50 mM Tris, 120 mM NaCl, 0.5% NP-40) were added to lysates and the samples rotated again for 1 h at 4 °C. After a wash in high salt buffer (50 mM Tris, 500 mM NaCl, 1% NP-40), the beads were washed twice with EBC buffer. Immunoprecipitates were eluted from beads by heating to 90 °C in Laemmli buffer for 3 min.

Arf6 activation assay. HEK293T cells were transfected with wildtype FLAG-IQSEC3 or with FLAG-IQSEC3 E749K. The Arf6 activation assay was performed as recommended by the vendor (Cytoskeleton Inc, USA; Cat. # BK033-S). For control, wildtype lysates were incubated with GDP or γsGTP for 15 min at 37°C and the reaction was stopped using the stop buffer provided by the vendor. The GGA3-PBD beads coupled to the Arf6 protein binding domain (PBD) of the effector protein GGA3 were added to all lysates for 45 min to enrich for activated Arf6 from the lysate. After washing twice in wash buffer, the denatured

samples were loaded onto SDS gels for WB analysis using the Arf6 monoclonal antibody provided by the vendor.

Calmodulin binding assay. HEK cells transfected with FLAG-tagged IQSEC3 constructs were lysed in the presence of either 2 mM $CaCl_2$ or 2 mM EGTA. To avoid decreasing $CaCl_2$ or EGTA concentrations in further steps in the assay, all solutions before elution contained either 2 mM $CaCl_2$ or 2 mM EGTA. After sparing a sample of each lysate as loading control, lysates were mixed with Calmodulin Sepharose beads (GE Halthcare, Little Chalfont, UK) and incubated on a rotator for 3 h at 4 °C. Beads were washed 3 times in 50 mM Tris, 150 mM NaCl, 1% Triton X-100 containing protease inhibitors (Complete Mini Protease Inhibitor Cocktail [Roche]). For elution, beads were incubated in 50 mM Tris, 150 mM NaCl containing high concentration of the opposite condition (10 mM EGTA or 10 mM $CaCl_2$) for 30 min at RT on a rotator. Supernatant containing pull-down proteins was mixed with Laemmli buffer, heated to 90 °C for 3 min and used for Western blot analysis.

Primary hippocampal cultures. Experiments were conducted in accordance with Swiss law on animal experimentation and the European Parliament Directive of 22 September 2010 on the protection of animals used for scientific purposes (2010/63/EU) and were approved by the cantonal veterinary office of Zurich. All measures were taken to minimize pain and suffering of the experimental animals. Specifically, pregnant Wistar rats (Charles River Laboratories, Germany; RRID:RGD_2308816) were anaesthetized at E18 with isoflurane (Attane; Piramal, Mumbai, India) (5% in air) until disappearance of pain reflexes (paw pinch) and sacrificed by cervical dislocation. Embryonic hippocampi were dissected on ice. Care was taken not to contaminate hippocampi with neocortical cells. After digestion of tissue with 0.5 mg/mL papain and 10 µg/mL DNase I for 15 min at 37 °C, cells were dissociated by gently mixing with a Pasteur pipette. Cells were diluted in DMEM + GlutaMAX-I (Thermo Fisher Scientific) including 10% FCS, 2 mM L-glutamine, 0.1 mg/mL gentamicin and 2.5 µg/mL fungizone and plated on poly-L-lysine-coated coverslips at a density of approximately 30'000 cells per coverslip. After 2 h incubation at 37 °C / 5% CO_2, coverslips were transferred to 12-well dishes containing cell culture medium (15 mM HEPES, 15% NU serum

[Corning Incorporated, Corning, NY], 0.45% glucose, 1 mM Na-pyruvate, 2 mM L-glutamine and B27 [1x; Thermo Fisher Scientific] in Minimum Essential Medium [Thermo Fisher Scientific]) and returned to the incubator until use.

Transfection of cultured neurons. Opti-MEM medium (Thermo Fisher Scientific) was mixed with 500 ng of endotoxin-free DNA per plasmid and coverslip to be transfected. After a 5 min incubation of lipofectamine 2000 (Oz Biosciences, Marseille, France) in Opti-MEM, the mix was added to the DNA solution for a final dilution of 1:30. Magnetofection reagent (Oz Biosciences) was added at a final dilution of 1:300 to the DNA / lipofectamine 2000 mixture and the solution was incubated at RT for 15 min. The transfection solution was added dropwise to coverslips in 1 mL of cell culture medium and cells incubated at 37 °C / 5% CO_2 for 40 min. Coverslips were transferred to 1 mL of conditioned medium and returned to the incubator until use.

Immunocytochemistry. Following a quick rinse in PBS to remove residual cell culture medium, cells were fixed immediately in 4% PFA in PBS for 10 min at RT. Coverslips were rinsed again in PBS and cells permeabilized in PBS containing 10% normal goat serum (NGS) and 0.15% Triton X-100 for 5 min. Cells were incubated with primary antibodies diluted in PBS containing 10% NGS for 90 min at RT. After washing coverslips 3 times in PBS for 5 min under agitation, cells were incubated with secondary antibodies diluted in PBS for 45 min. Secondary antibodies were raised in goat and were coupled to the following fluorophores: Alexa Fluor 488 (1:1000; Jackson ImmunoResearch, West Grove, PA), Cy3 (1:500; Jackson ImmunoResearch), Alexa Fluor 647 (1:1000; Jackson ImmunoResearch). Coverslips were washed 3 times in PBS for 5 min under agitation, dried and mounted with Fluorescence Mounting Medium (Dako, Carpinteria, CA).

Image acquisition and analysis. All specimens from neuronal cultures were imaged using confocal laser scanning microscopy (LSM 700 and LSM 710, Carl Zeiss, Oberkochen, Germany). Images were taken using a 40x objective with a numerical aperture of 1.4 and had a pixel size of 112 x 112 nm^2. For quantification of synaptic markers, individual dendrites were framed by a region of interest with 2.5 µm thickness and clusters (representing pre- or

postsynaptic protein aggregates) were quantified by an automated macro in ImageJ (NIH, Bethesda, MD). To determine apposition of pre- and postsynaptic clusters, presynaptic marker size was enlarged by 1 pixel and colocalization with postsynaptic markers sampled. All imaging and quantification parameters were kept constant between conditions.

Experimental design and statistical analysis. This study was not pre-registered due to its explorative nature. All plasmids used for one given experiment were transfected in cells derived from a single cell preparation (pooled from all embryos prepared) and all experiments were repeated at least three times. Coverslips were selected at random prior to transfection. In each experiment, data were collected from multiple dendrites and regions of interest in each cell. Statistical analysis of cluster density values was performed with averaged data points from individual cells; cluster size values were compared from pooled cluster data from all cells per group (Tables 1 and 2). No power analysis was performed owing to the nested nature of the data (coverslips-cells-regions of interest). All quantifications involving mutant constructs were performed by an observer unaware of the type of construct transfected.

Statistical tests were performed using Prism software (GraphPad, La Jolla, CA). Data points in cluster density graphs represent individual cells and whiskers indicate standard error of the mean. One-way ANOVA and Kruskal-Wallis tests were used for analyzing differences in cluster density and cluster size, respectively. The threshold for significance was set at $P < 0.05$.

Results

IQSEC3 was described as a dystrophin-interacting protein because of its capability to bind dystrophin WW domains and due to the colocalization of both proteins in primary hippocampal neurons (Fukaya et al. 2011). Immunohistochemical analyses of brain and retina sections, however, revealed a distribution pattern reminiscent of more broadly distributed proteins of the GABAergic PSD, such as gephyrin (Fukaya et al. 2011, Sakagami et al. 2013). For this reason, we probed IQSEC3-gephyrin interaction in heterologous cells. According to known functions of domains found in IQSEC3 homologs, mutations and

truncations of FLAG-tagged IQSEC3 were generated and co-expressed with eGFP-tagged gephyrin in HEK293T cells (Figure 1). Gephyrin was found to co-immunoprecipitate with wildtype IQSEC3. Mutation of the IQ motif (I318A/Q319A/R323A), a serine residue undergoing phosphorylation (S348), the catalytically essential glutamate residue in Sec7 domain (E749K) or the dystrophin-interacting PP motif (P1165A/P1166A/Y1168A) had no effect on gephyrin binding efficiency (Figure 1B and C) (Fukaya et al. 2011, Trinidad *et al.* 2006, Cherfils et al. 1998, Myers et al. 2012). Interaction with gephyrin was also retained when using a IQSEC3 construct lacking the pleckstrin homology (PH) domain (Figure 1B). However, deletion of the first N-terminal 181 amino acids in IQSEC3 caused a drastic reduction of eGFP-gephyrin detected in the immunoprecipitate (Figure 1C and E). In order to determine the minimal domain requirement of IQSEC3 for gephyrin interaction, various IQSEC3 truncations were probed for the ability to co-immunoprecipitate gephyrin. Surprisingly, the coiled coil 1 (CC1)-containing N-terminal part alone was not able to bind gephyrin, but the domain containing the IQ motif was sufficient for gephyrin binding (Figure 1D). Within the IQ motif-containing domain, the region close to the IQ motif was found to bind gephyrin, whereas the region close to the Sec7 domain did not (Figure 1E). Expression of an intermediate region (IQ fragment 2) and of the isolated Sec7 domain was not strong enough to assess binding capability to gephyrin. Together, these results show that IQSEC3 binds to gephyrin near the IQ motif and that the N-terminal CC domain is required for efficient binding. To verify that the E749K mutation abolishes catalytic activity of Sec7 mutant, an Arf6 activation assay was used in transfected HEK cells. As expected, levels of activated Arf6 pulled down by Arf6-PBD beads were much lower when Sec7 mutant was overexpressed compared to wildtype, demonstrating that the E749K mutation interferes with the catalytic activity of IQSEC3 (Figure 2A). Because co-IP results pointed to an interaction of gephyrin with IQSEC3 near its IQ motif, the functional importance of the IQ motif in IQSEC3 was examined using a calmodulin binding assay. IQSEC3 constructs were expressed in HEK293T cells and lysates incubated with calmodulin-bound beads either in the presence of 2 mM Ca^{2+} or 2 mM EGTA. Indeed, binding of IQSEC3 to calmodulin was observed in low

Ca^{2+} conditions (Figure 2B). This interaction was completely abolished for the IQSEC3 IQ mutant, but not for the Sec7 mutant or the ΔN construct, confirming that binding takes place at the IQ motif.

Similar to glutamate receptor regulation by IQSEC3 homologs IQSEC1 and IQSEQ2, the role of IQSEC3 at GABAergic PSD might depend on its catalytic function (Myers et al. 2012, Scholz et al. 2010). To test this possibility, FLAG-tagged IQSEC3 constructs were overexpressed in primary hippocampal neurons together with eGFP-gephyrin at DIV 8 and analyzed at DIV 15 (DIV 8+7). Overexpressed IQSEC3 variants largely colocalized with eGFP-gephyrin but were also diffusely distributed in dendrites and the cell soma (Figure 3A). Cultures were labeled with anti-VGAT or anti-VGluT1+2 antibodies to distinguish between GABAergic synapses and mismatched synapses (gephyrin clusters apposed to glutamatergic terminals). This approach revealed a dramatic elevation of eGFP-gephyrin clusters non-apposed to VGAT-positive terminals in cells overexpressing IQSEC3 Sec7 mutant in comparison to cells transfected with empty vector or with other IQSEC3 constructs (Figure 3A and B). A reduction of the percentage of VGAT-apposed gephyrin clusters paralleled the cluster density results in Sec7 mutant-overexpressing cells. The density of eGFP-gephyrin clusters apposed to VGluT1+2-positive terminals was increased to a similar extent as the VGAT non-apposed gephyrin cluster density, demonstrating that many VGAT non-apposed clusters were mismatched (Figure 3C). Sec7 mutant-transfected cells also exhibited an increase in overall eGFP-gephyrin cluster density, consistent with the notion that Sec7 mutant overexpression promotes mismatched gephyrin clustering (Figure 3D). Surprisingly, overexpression of wildtype IQSEC3 and IQ motif mutant did not lead to changes in overall eGFP-gephyrin cluster density or in apposition of eGFP-gephyrin clusters. Finally, eGFP-gephyrin cluster size was reduced in cells transfected with any of the IQSEC3 constructs, indicating that this reduction is caused by binding of constructs to gephyrin and not by IQSEC3 catalytic activity (Figure 3E).

IQSEC3 exhibits a PDZ domain-binding motif at the C-terminal end and was first described as a protein enriched in the PSD of glutamatergic synapses (Inaba et al. 2004). The

observed phenotype could be a manifestation of a more general function of IQSEC3 in synapse validation, both for GABAergic and glutamatergic PSD proteins. For this reason, we co-expressed IQSEC3 constructs with GFP-PSD-95 and examined apposition to presynaptic markers (Figure 4). In contrast to eGFP-gephyrin, GFP-PSD-95 did not preferentially colocalize with FLAG-IQSEC3 constructs when co-expressed (Figure 4A). Also, IQSEC3 catalytic function did not affect the density of mismatched (VGAT-apposed) PSD-95 clusters. GFP-PSD-95 clusters were about 5 times more frequently apposed to VGluT1+2- than to VGAT-positive terminals in all conditions (Figure 4A-D). In addition, GFP-PSD-95 cluster size was not affected by overexpression of IQSEC3 constructs (Figure 4E). IQSEC3 catalytic function thus seems to be specifically required for regulation of presynaptic terminal apposition to the GABAergic PSD.

Regulation of gephyrin presynaptic apposition by IQSEC3 raises the question whether such control is exerted through trans-synaptic signaling or whether purely postsynaptic mechanisms are involved. Quantification of presynaptic marker density revealed that innervation density is not affected by IQSEC3 overexpression (Figure 5). In terms of fraction of presynaptic markers apposed to eGFP-gephyrin, only VGluT1+2 puncta exhibited an increase upon Sec7 mutant overexpression. This observation is consistent with the notion that IQSEC3 has a postsynaptic role in regulation of mismatched synapses.

To exclude the possibility that IQSEC3 function is restricted to downregulation of gephyrin at mismatched sites, overexpression experiments were repeated without eGFP-gephyrin co-expression. Instead, $GABA_AR$ γ2 subunit was immunolabeled to assess consequences of IQSEC3 wildtype and Sec7 mutant overexpression for $GABA_AR$ apposition (Figure 6). Neighboring untransfected dendrites were used in both conditions as internal controls. As with eGFP-gephyrin co-expression, Sec7 mutant-transfected cells exhibited a higher proportion of mismatched γ2 subunit clusters (apposed to VGluT1+2-positive terminals) than untransfected dendrites. Along with gephyrin apposition, IQSEC3 catalytic function thus contributes to regulate the apposition of $GABA_AR$ clusters to neurotransmitter-specific presynaptic terminals.

If Arf6 is the target of IQSEC3 catalytic activity for regulation of GABAergic PSD apposition, abolition of Arf6 activity alone should replicate the apposition phenotype of the Sec7 mutant. Overexpression of Arf6 in its wildtype form, and to a larger extent overexpression of constitutively active (CA; Q67L) or dominant negative (DN; T27N) Arf6 mutants, affects neuronal morphology (Hernandez-Deviez *et al.* 2002, Miyazaki *et al.* 2005). Neurite and spine outgrowth seem to be regulated by Arf6, since these processes are promoted by Arf6 DN and inhibited by Arf6 CA overexpression, respectively. For this reason, primary hippocampal neurons overexpressing HA-tagged Arf6 variants were probed with antibodies to $GABA_AR$ α2 subunit to ensure that formation of the GABAergic PSD is not affected by morphological changes. The α2 subunit was selected for analysis, rather than γ2, because it more distinctly labels postsynaptic $GABA_AR$ clusters. As expected, $GABA_AR$ α2 subunit clusters were observed on dendrites of Arf6-expressing neurons to the same extent as on non-transfected neurons (Figure 7A). To facilitate the assessment of GABAergic PSD abundance and apposition patterns, eGFP-gephyrin was co-expressed with Arf6 constructs. As expected from observations of $GABA_AR$ α2 subunit clustering, the overall density of eGFP-gephyrin clusters did not change upon Arf6 construct overexpression (Figure 7B). Analysis of presynaptic apposition, however, uncovered that in Arf6 DN-expressing cells a smaller fraction of eGFP-gephyrin clusters was correctly apposed and a larger fraction was present in mismatched synapses, both compared to Arf6 CA-expressing cells and to cells expressing eGFP-gephyrin only (Figure 7C-D). Similar to results from IQSEC3 overexpression experiments, these alterations were caused by an increase in the proportion of mismatched gephyrin clusters apposed to VGluT1+2-positive terminals. Therefore, Arf6 activity is sufficient for regulation of apposition between the GABAergic PSD and presynaptic terminals, indicating that Arf6 activation by IQSEC3 is involved in this process.

The N-terminal CC1-containing domain necessary for gephyrin interaction in IQSEC3 has been demonstrated to be essential for homomultimerization in IQSEC2 (Myers et al. 2012). This line of evidence suggests a relationship between IQSEC3 homomultimerization and gephyrin interaction. However, the N-terminal CC1-containing domain is dispensable for

homomultimerization in IQSEC3, as assessed by co-immunoprecipitation of mCherry-tagged with FLAG-tagged IQSEC3 variants (Figure 8A). Of all constructs tested, only mutation of S348 to alanine modulated the proportion of co-immunoprecipitated mCherry-tagged IQSEC3, raising the possibility that phosphorylation of this residue is involved in regulating IQSEC3 homomultimerization.

FLAG-tagged IQSEC3 overexpressed in primary hippocampal neurons formed large somatic aggregates, reminiscent of aggregates formed by overexpressed eGFP-gephyrin (Figure 8B). These somatic IQSEC3 aggregates were consistently immunopositive for endogenous gephyrin. Deletion and mutation constructs of IQSEC3 were tested for their ability to form somatic aggregates. Strikingly, deletion of the N-terminus abolished the majority of somatic aggregates and so did mutation of the IQ motif. Mutation of S348, the catalytic glutamate residue in the Sec7 domain, the PP motif or deletion of the PH domain did not influence somatic IQSEC3 aggregation. Since individual domains did not form aggregates, somatic aggregates might be formed only by IQSEC3 constructs retaining gephyrin and calmodulin interaction capability. Together, these results suggest that IQSEC3 function is mediated by interactions with gephyrin and calmodulin.

Discussion

Our study of IQSEC3 function in primary hippocampal neurons provides evidence for control of mismatched GABAergic PSD proteins by IQSEC3, in a mechanism that likely depends on Ca^{2+}-calmodulin signaling. Catalytic activity is implicated in this regulation by the strong effect of Sec7 domain mutation as well as the recapitulation of the misapposition phenotype by Arf6 overexpression. IQSEC3 function is restricted to mis-apposed GABAergic PSDs since PSD-95 apposition to GABAergic or glutamatergic terminals was not affected, suggesting that the interaction with gephyrin might be implicated in regulating IQSEC3 function. Moreover, Ca^{2+}-dependent calmodulin binding and the finding that correctly matched GABAergic PSDs were unaffected in all experiments strongly suggests that proximity to glutamatergic structures enables this function of IQSEC3. Gephyrin binding near the calmodulin binding site and calmodulin binding were found to be essential for somatic aggregation of overexpressed

IQSEC3. This observation points to a mechanism by which IQSEC3 undergoes conformational changes upon neuronal activity and gephyrin binding to regulate mismatched GABAergic PSD proteins.

A physiologically relevant interaction of IQSEC3 with gephyrin is suggested by several findings. First, co-IP experiments in heterologous cells revealed binding that depended on domains with known functions. Secondly, co-expression of both proteins in primary neurons led to extensive colocalization in all subcellular domains. Thirdly, somatic IQSEC3 aggregates formed upon overexpression were immunopositive for endogenous gephyrin. These observations are in line with the extensive colocalization of IQSEC3 with markers of GABAergic synapses reported in various parts of the CNS (Fukaya et al. 2011, Sakagami et al. 2013). Dystrophin interaction may be involved in accumulating IQSEC3 at dystrophin-containing synapses. However, the restricted dystrophin distribution in cortical areas excludes an obligatory role for dystrophin in IQSEC3 clustering (Lidov *et al.* 1990, Knuesel *et al.* 1999). Along the same lines, localization of IQSEC3 containing mutated PP motif, which is necessary for dystrophin interaction, did not differ from wildtype and IQSEC3 clustering was virtually unaffected in the hippocampus of mice with pyramidal cell-specific loss of the dystrophin-glycoprotein complex (Fruh *et al.* 2016). Gephyrin binding to IQSEC3 was reported on the basis of yeast-two-hybrid and co-IP experiments and also identified the IQ motif area as the minimally-required area for interaction (Um *et al.* 2016). Furthermore, gephyrin downregulation in primary neurons caused a reduction in IQSEC3 clustering, arguing that this interaction is necessary for IQSEC3 synaptic localization. Substantial evidence has thus accumulated that IQSEC3 is enriched in the GABAergic PSD due to specific gephyrin interaction near the IQ motif.

Paradoxically, Um et al. (2016) have found an overall increase of gephyrin and GAD67 puncta density upon IQSEC3 overexpression, an effect which was dependent on gephyrin binding as well as on IQSEC3 catalytic activity. The reasons for the discrepancy to our results are not clear, since the same isoform of rat IQSEC3 was used in primary hippocampal cultures. Still, the use of the chicken beta-actin enhancer by Um et al. and the

resulting strong overexpression of IQSEC3 might explain some of the differences. None of our experiments have yielded results that implicate IQSEC3 in the regulation of correctly apposed GABAergic proteins, despite the preferential GABAergic localization of IQSEC3. Further experiments will have to clarify whether IQSEC3 can contribute to overall GABAergic synapse development, and under what conditions.

Interaction with gephyrin might reflect a mechanism to target IQSEC3 to the GABAergic PSD rather than an interaction implicating direct gephyrin regulation. Indeed, gephyrin binding might even have an inhibitory effect on IQSEC3 catalytic activity, since IQSEC3 seems to be catalytically inactive in correctly apposed GABAergic PSDs. Other factors must be present at mismatched sites which promote IQSEC3 activity. Ca^{2+} is a likely candidate to take this role, because of calmodulin binding near the gephyrin-binding site in low Ca^{2+} conditions. The release of calmodulin from IQSEC3 at high Ca^{2+} concentrations might enable an active conformational state allowing activation of Arf6 in the mismatched GABAergic PSD. Involvement of calmodulin in formation of such an active state would also account for the fact that neuronal activity was implicated in the fidelity of GABAergic apposition (Anderson et al. 2004). Mutation of S348 to alanine increased the capacity of IQSEC3 to multimerize but did not directly affect gephyrin binding in co-IP experiments. Since this residue was found to be phosphorylated in PSD fraction (Trinidad *et al.* 2006), it will be important to clarify whether S348 phosphorylation serves to regulate IQSEC3 catalytic activity.

The fact that Arf6 catalytic mutants replicated the misapposition phenotype of the Sec7 mutant strongly suggests that Arf6 acts as a substrate of IQSEC3 in this context. Arf6 is also the target of IQSEC1 and IQSEC2, leading to the internalization of GluA2 and GluA1 subunits, respectively. In order for IQSEC3 to achieve GABAergic PSD-specific regulation, activation of Arf6 would have to be restricted to GABAergic PSD-containing nanodomains. It is unclear how this specificity is ensured in mismatched synapses, presumably containing glutamatergic PSD proteins in addition to GABAergic PSD proteins, but spatial restriction of IQSEC3 to specific subdomains of the PSD might be one level of control. Arf6 is a membrane-bound GTPase which has diverse functions in neurons and is controlled by a

multitude of GEF and GTPase-activating proteins (Jaworski 2007). Downstream effectors of Arf6 regulate actin dynamics and both clathrin-dependent and -independent plasma membrane endocytosis. Therefore, direct regulation of gephyrin clustering, as well as regulation of PSD proteins through internalization of $GABA_A$Rs, are possible consequences of IQSEC3-mediated activation of Arf6, which might eventually lead to the elimination of a mismatched synapse.

The absence of spatial and temporal cues is likely the main underlying cause for the formation of mismatched synapses in primary neuronal cultures. Therefore, it is unclear whether the regulation of misapposition by IQSEC3 has a physiological relevance *in vivo*. However, it is conceivable that formation of mismatched synapses by loss of guidance cues follows different principles than what was uncovered by overexpression of the Sec7 mutant. This notion is supported by the observation that overexpression of wildtype IQSEC3 did not lead to a statistically significant reduction of mismatched synapses, since mismatched synapses caused by other mechanisms might not be under the influence of IQSEC3 regulation. *In vivo*, IQSEC3 function might be restricted to synapses that are closely apposed to synapses employing a different neurotransmitter system. GABAergic synapses that are located on dendritic spines are often in close proximity to glutamatergic synapses and therefore IQSEC3 might be involved in the regulation of spine PSD nanodomains (Chen *et al.* 2012, van Versendaal *et al.* 2012). Although complicated by high synaptic density *in vivo*, increased focus on synaptic mismatch in intact tissue might thus lead to a better understanding of the mechanisms underlying neurotransmitter-specific PSD regulation. On the one hand, IQSEC3 knockout mice will be instrumental in the elucidation of the physiological roles of IQSEC3. On the other hand, the development of *in vivo* models of synaptic mismatch would allow probing the involvement of genes required to correct misapposition, by designing rescue experiments. This might be achievable through blockade of neuronal activity, as mismatch of GABAergic terminals with glutamatergic postsynaptic structures was observed in Purkinje cells of TTX-infused cerebella (Cesa *et al.* 2008), replicating the effects seen in the absence of $GABA_A$R (Fritschy et al. 2006). However, to the

best of our knowledge, occurrence of postsynaptic GABAergic structures mis-apposed to glutamatergic axon terminals was not yet demonstrated *in vivo*.

Strikingly, in a post-mortem transcriptomic analysis of human cortex, IQSEC3 was found to be the gene which is most strongly downregulated across schizophrenia, autism and bipolar disorder (Ellis *et al.* 2016). Major issues that have to be addressed on the path to potential translational applications of our findings include the question of Arf subtype activation of human IQSEC3 and the uncertainty of mismatch-regulating mechanisms *in vivo*. So far, the physiological and behavioral consequences of receptor-transmitter mismatch *in vivo* are unexplored. However, in the light of association of IQSEC3 expression levels with major psychiatric disorders in humans, a role for synaptic mismatch in the etiology of these disorders should be considered in future investigations.

Acknowledgements

The authors have no conflict of interest to declare. This work was supported by a University of Zurich Forschungskredit grant to S.F. and by the Swiss National Science Foundation (Grant 310030_146120 to JMF). We thank Dr. Hiroyuki Sakagami for providing reagents and Prof. Peter Scheiffele and Prof. Stephan Neuhauss for scientific discussions. The authors declare no competing financial interests.

References

Anderson, T. R., Shah, P. A. and Benson, D. L. (2004) Maturation of glutamatergic and GABAergic synapse composition in hippocampal neurons. *Neuropharmacology,* **47,** 694-705.

Bähler, M. and Rhoads, A. (2002) Calmodulin signaling via the IQ motif. *FEBS Lett,* **513,** 107-113.

Brunig, I., Suter, A., Knuesel, I., Luscher, B. and Fritschy, J. M. (2002) GABAergic terminals are required for postsynaptic clustering of dystrophin but not of GABA(A) receptors and gephyrin. *J Neurosci,* **22,** 4805-4813.

Caroni, P., Chowdhury, A. and Lahr, M. (2014) Synapse rearrangements upon learning: from divergent-sparse connectivity to dedicated sub-circuits. *Trends Neurosci,* **37,** 604-614.

Cesa, R., Morando, L. and Strata, P. (2008) Transmitter-receptor mismatch in GABAergic synapses in the absence of activity. *Proc Natl Acad Sci U S A,* **105,** 18988-18993.

Chen, J. L., Villa, K. L., Cha, J. W., So, P. T., Kubota, Y. and Nedivi, E. (2012) Clustered dynamics of inhibitory synapses and dendritic spines in the adult neocortex. *Neuron,* **74,** 361-373.

Cherfils, J., Menetrey, J., Mathieu, M., Le Bras, G., Robineau, S., Beraud-Dufour, S., Antonny, B. and Chardin, P. (1998) Structure of the Sec7 domain of the Arf exchange factor ARNO. *Nature,* **392,** 101-105.

Christie, S. B., Miralles, C. P. and De Blas, A. L. (2002) GABAergic innervation organizes synaptic and extrasynaptic GABAA receptor clustering in cultured hippocampal neurons. *J Neurosci,* **22,** 684-697.

Ellis, S. E., Panitch, R., West, A. B. and Arking, D. E. (2016) Transcriptome analysis of cortical tissue reveals shared sets of downregulated genes in autism and schizophrenia. *Transl Psychiatry,* **6,** e817.

Fritschy, J. M. and Mohler, H. (1995) GABAA-receptor heterogeneity in the adult rat brain: differential regional and cellular distribution of seven major subunits. *J Comp Neurol,* **359,** 154-194.

Fritschy, J. M., Panzanelli, P., Kralic, J. E., Vogt, K. E. and Sassoe-Pognetto, M. (2006) Differential dependence of axo-dendritic and axo-somatic GABAergic synapses on GABAA receptors containing the alpha1 subunit in Purkinje cells. *J Neurosci,* **26,** 3245-3255.

Fruh, S., Romanos, J., Panzanelli, P., Burgisser, D., Tyagarajan, S. K., Campbell, K. P., Santello, M. and Fritschy, J. M. (2016) Neuronal Dystroglycan Is Necessary for Formation and Maintenance of Functional CCK-Positive Basket Cell Terminals on Pyramidal Cells. *J Neurosci,* **36,** 10296-10313.

Fukaya, M., Kamata, A., Hara, Y. et al. (2011) SynArfGEF is a guanine nucleotide exchange factor for Arf6 and localizes preferentially at post-synaptic specializations of inhibitory synapses. *J Neurochem,* **116,** 1122-1137.

Hattori, Y., Ohta, S., Hamada, K., Yamada-Okabe, H., Kanemura, Y., Matsuzaki, Y., Okano, H., Kawakami, Y. and Toda, M. (2007) Identification of a neuron-specific human gene, KIAA1110, that is a guanine nucleotide exchange factor for ARF1. *Biochem Biophys Res Commun,* **364,** 737-742.

Hernandez-Deviez, D. J., Casanova, J. E. and Wilson, J. M. (2002) Regulation of dendritic development by the ARF exchange factor ARNO. *Nat Neurosci,* **5,** 623-624.

Inaba, Y., Tian, Q. B., Okano, A. et al. (2004) Brain-specific potential guanine nucleotide exchange factor for Arf, synArfGEF (Po), is localized to postsynaptic density. *J Neurochem,* **89,** 1347-1357.

Jaworski, J. (2007) ARF6 in the nervous system. *Eur J Cell Biol,* **86,** 513-524.

Khazipov, R., Esclapez, M., Caillard, O. et al. (2001) Early development of neuronal activity in the primate hippocampus in utero. *J Neurosci,* **21,** 9770-9781.

Kikuno, R., Nagase, T., Ishikawa, K., Hirosawa, M., Miyajima, N., Tanaka, A., Kotani, H., Nomura, N. and Ohara, O. (1999) Prediction of the coding sequences of unidentified human genes. XIV. The complete sequences of 100 new cDNA clones from brain which code for large proteins in vitro. *DNA Res,* **6,** 197-205.

Knuesel, I., Mastrocola, M., Zuellig, R. A., Bornhauser, B., Schaub, M. C. and Fritschy, J. M. (1999) Short communication: altered synaptic clustering of GABAA receptors in mice lacking dystrophin (mdx mice). *Eur J Neurosci,* **11,** 4457-4462.

Lidov, H. G., Byers, T. J., Watkins, S. C. and Kunkel, L. M. (1990) Localization of dystrophin to postsynaptic regions of central nervous system cortical neurons. *Nature,* **348,** 725-728.

Missler, M., Sudhof, T. C. and Biederer, T. (2012) Synaptic cell adhesion. *Cold Spring Harb Perspect Biol,* **4,** a005694.

Miyazaki, H., Yamazaki, M., Watanabe, H., Maehama, T., Yokozeki, T. and Kanaho, Y. (2005) The small GTPase ADP-ribosylation factor 6 negatively regulates dendritic spine formation. *FEBS Lett,* **579,** 6834-6838.

Mossessova, E., Gulbis, J. and Goldberg, J. (1998) Structure of the guanine nucleotide exchange factor Sec7 domain of human arno and analysis of the interaction with ARF GTPase. *Cell,* **92,** 415-423.

Myers, K. R., Wang, G., Sheng, Y., Conger, K. K., Casanova, J. E. and Zhu, J. J. (2012) Arf6-GEF BRAG1 regulates JNK-mediated synaptic removal of GluA1-containing AMPA receptors: a new mechanism for nonsyndromic X-linked mental disorder. *J Neurosci,* **32,** 11716-11726.

Rao, A., Cha, E. M. and Craig, A. M. (2000) Mismatched appositions of presynaptic and postsynaptic components in isolated hippocampal neurons. *J Neurosci,* **20,** 8344-8353.

Sakagami, H., Katsumata, O., Hara, Y., Tamaki, H., Watanabe, M., Harvey, R. J. and Fukaya, M. (2013) Distinct synaptic localization patterns of brefeldin A-resistant guanine nucleotide exchange factors BRAG2 and BRAG3 in the mouse retina. *J Comp Neurol,* **521,** 860-876.

Scholz, R., Berberich, S., Rathgeber, L., Kolleker, A., Kohr, G. and Kornau, H. C. (2010) AMPA receptor signaling through BRAG2 and Arf6 critical for long-term synaptic depression. *Neuron,* **66,** 768-780.

Trinidad, J. C., Specht, C. G., Thalhammer, A., Schoepfer, R. and Burlingame, A. L. (2006) Comprehensive identification of phosphorylation sites in postsynaptic density preparations. *Mol Cell Proteomics,* **5,** 914-922.

Tyzio, R., Represa, A., Jorquera, I., Ben-Ari, Y., Gozlan, H. and Aniksztejn, L. (1999) The establishment of GABAergic and glutamatergic synapses on CA1 pyramidal neurons is sequential and correlates with the development of the apical dendrite. *J Neurosci,* **19,** 10372-10382.

Um, J. W., Choii, G., Park, D. et al. (2016) IQ Motif and SEC7 Domain-containing Protein 3 (IQSEC3) Interacts with Gephyrin to Promote Inhibitory Synapse Formation. *J Biol Chem,* **291,** 10119-10130.

van Versendaal, D., Rajendran, R., Saiepour, M. H. et al. (2012) Elimination of inhibitory synapses is a major component of adult ocular dominance plasticity. *Neuron,* **74,** 374-383.

Figure legends

Figure 1

IQSEC3 interacts with gephyrin G- or C-domain near the IQ motif. A, Schematic overview of IQSEC3 constructs and summary of gephyrin interaction results. Binding to gephyrin is indicated by "+", "(+)" indicates weaker binding compared to wildtype IQSEC3 and "-" indicates absence of binding. B-E, Representative Western blots of co-immunoprecipitation (co-IP) experiments performed to assess IQSEC3 interaction with gephyrin. In all experiments, constructs were expressed in HEK293T cells and lysates used for co-IP using mouse anti-FLAG antibody bound to agarose beads. Two negative controls were employed to exclude unspecific binding. Anti-FLAG antibody was replaced by unspecific mouse IgG but both constructs were expressed. In addition, the construct to be immunoprecipitated was not expressed but immunoprecipitation antibody was present. B, Mutation of IQ motif, Sec7 catalytic domain and PP motif, as well as deletion of PH domain, do not hinder binding of IQSEC3 to gephyrin. C, Mutation of IQSEC3 S348 does not affect binding to gephyrin but N-terminal CC domain is necessary for efficient interaction with gephyrin. D, IQ domain is sufficient for gephyrin binding and CC domain, which is missing in N-terminal deletion, itself does not bind gephyrin. For constructs encoding Sec7 domain and Sec7 domain containing E749K mutation (Sec7 mutant) expression in HEK293T cells was too week to assess interaction by co-IP. E, Gephyrin binds to a region near the IQ motif in IQSEC3. IQ fragment 1 was detected in immunoprecipitates but not IQ fragment 3. Expression of IQ fragment 2 in HEK293T cells was too weak to assess binding to gephyrin.

Figure 2

Validation of functional significance of IQSEC3 mutations. A, Arf6 activation assay demonstrating that E749K mutation abolishes activation of Arf6 by IQSEC3. The upper blot depicts Arf6 immunoreactivity following pull-down of activated Arf6. The lower blot is the loading control. B, Apocalmodulin binds to IQSEC3 IQ motif. Representative Western blot of calmodulin pull-down of IQSEC3 constructs in high and low Ca^{2+} conditions. IQSEC3 binds

to calmodulin more efficiently in low Ca2+ conditions and requires IQ motif for interaction. IQSEC3 constructs were overexpressed in HEK293T cells and lysates used for calmodulin pull-down assay in the presence of 2 mM $CaCl_2$ or 2 mM EGTA.

Figure 3

The catalytic function of IQSEC3 regulates apposition of gephyrin to presynaptic terminals. FLAG-tagged IQSEC3 constructs or an empty vector were co-expressed with eGFP-gephyrin in primary hippocampal neurons at DIV 8 and apposition to VGAT or VGluT1+2 immunofluorescent puncta assessed at DIV 15. A, Representative images of dendrites of transfected cells. FLAG immunoreactivity is shown in cells co-labeled for VGAT. IQSEC3 Sec7 mutant-overexpressing cells exhibit an increased amount of VGAT-non-apposed eGFP-gephyrin clusters (arrowheads) in comparison to all other constructs. VGluT1+2-apposed eGFP-gephyrin clusters (arrows) are also more abundant in cells overexpressing Sec7 mutant. B, Quantification of eGFP-gephyrin VGAT apposition. VGAT-apposed eGFP-gephyrin cluster density was not significantly different between constructs. In contrast, VGAT-non-apposed eGFP-gephyrin clusters displayed an increased density in Sec7 mutant-expressing cells compared to all other constructs, resulting in a decreased percentage of VGAT-apposed eGFP-gephyrin clusters. C, Quantification of eGFP-gephyrin VGluT1+2 apposition. VGluT1+2-apposed eGFP-gephyrin cluster density was increased by overexpression of Sec7 mutant but in VGluT1+2-non-apposed eGFP-gephyrin clusters no significant differences were found between groups. The increase of VGluT1+2-apposed eGFP-gephyrin cluster density in Sec7 mutant-expressing neurons is reflected in a higher percentage of VGluT1+2-apposed eGFP-gephyrin clusters. D, Quantification of total dendritic eGFP-gephyrin cluster densities. Overexpression of IQSEC3 Sec7 mutant led to an increase in eGFP-gephyrin cluster density whereas IQSEC3 wildtype or IQ mutant did not significantly change eGFP-gephyrin cluster density. E, Quantification of overall eGFP-gephyrin cluster size in cells co-expressing IQSEC3 constructs. Compared to empty vector, all IQSEC3 constructs caused a small but statistically significant reduction of cluster size when co-expressed with eGFP-gephyrin. In box plots, lines, crosses, boxes and whiskers represent

median, mean, 25-75 percentile and 10-90 percentile, respectively. Data points represent individual cells. **p<0.01, ***p<0.001; (see Tables 1-2 for results of statistical analyses).

Figure 4

IQSEC3 catalytic function is not involved in regulation of presynaptic apposition of glutamatergic postsynaptic density. FLAG-tagged IQSEC3 constructs were co-expressed with GFP-PSD-95 in primary hippocampal neurons at DIV 8 and apposition to presynaptic markers analyzed at DIV 15. A, Representative images of dendrites of transfected cells immunolabeled either for VGAT or VGluT1+2. FLAG immunoreactivity is shown in cells co-labeled for VGAT. The majority of GFP-PSD-95 clusters is apposed to VGluT1+2 puncta but a minor fraction of clusters is mis-apposed to VGAT (arrows) or is not apposed to VGluT1+2 (arrowheads). B-E, Quantification of clustering and apposition parameters of GFP-PSD-95. In all analyses, there were no statistically significant differences found between constructs. B, Quantification of VGAT apposition of GFP-PSD-95. C, Quantification of VGluT1+2 apposition of GFP-PSD-95. D, Quantification of total dendritic GFP-PSD-95 cluster densities. E, Quantification of overall GFP-PSD-95 cluster size. In box plots, lines, crosses, boxes and whiskers represent median, mean, 25-75 percentile and 10-90 percentile, respectively. Data points represent individual cells; (see Tables 1-2 for results of statistical analyses).

Figure 5

Fraction of mismatched glutamatergic presynaptic terminals but not innervation density is affected by IQSEC3 catalytic function. A, Quantification of VGAT puncta densities and percentage of VGAT puncta apposed to eGFP-gephyrin. Co-expression of IQSEC3 constructs had no statistically significant effect on puncta density or percentage of apposition to eGFP-gephyrin. B, Quantification of VGluT1+2 puncta densities and percentage of VGluT1+2 puncta apposed to eGFP-gephyrin. Percentage of VGluT1+2 puncta apposed to eGFP-gephyrin was increased in Sec7 mutant-overexpressing cells compared to all other groups but absolute VGluT1+2 densities were unaffected by IQSEC3 construct co-

expression. Data points represent individual cells. ***p<0.001; (see Table 1 for results of statistical analyses).

Figure 6

Presynaptic apposition of $GABA_A$ receptors is regulated by IQSEC3 catalytic function. Primary hippocampal neurons were transfected with IQSEC3 wildtype or Sec7 mutant constructs at DIV 8 and presynaptic apposition of $GABA_AR$ γ2 subunit clusters analyzed at DIV 15. Untransfected dendrites neighboring transfected cells served as control. A, Representative images of dendrites of cells transfected with IQSEC3 constructs (upper panels; FLAG immunolabeling shown) and untransfected neighboring dendrites (lower panels) immunolabeled for VGAT. Note the high abundance of $GABA_AR$ γ2 subunit clusters not apposed to VGAT (arrowheads) in dendrites of cells transfected with Sec7 mutant. B, Quantification of $GABA_AR$ γ2 subunit cluster VGAT apposition. Compared to untransfected neighboring dendrites and to cells overexpressing wildtype IQSEC3, cells overexpressing Sec7 mutant show elevated VGAT-non-apposed cluster densities, reflected in a lower percentage of VGAT-apposed clusters. C, Representative images of dendrites of cells transfected with IQSEC3 constructs (upper panels; FLAG immunolabeling shown) and untransfected neighboring dendrites (lower panels) immunolabeled for VGluT1+2. Note the high abundance of $GABA_AR$ γ2 subunit clusters apposed to VGluT1+2 puncta (arrows) in dendrites of cells overexpressing Sec7 mutant. D, Quantification of $GABA_AR$ γ2 subunit cluster VGluT1+2 apposition. Sec7 mutant-transfected cells showed significantly higher density of VGluT1+2-apposed $GABA_AR$ γ2 subunit clusters compared to untransfected cells and to cells transfected with wildtype IQSEC3. The increase in VGluT1+2-apposed cluster density is mirrored by a higher percentage of VGluT1+2-apposed clusters. Data points represent individual cells. *p<0.05, **p<0.01, ***p<0.001; (see Table 1 for results of statistical analyses).

Figure 7

Arf6 is involved in regulation of gephyrin presynaptic apposition. A, $GABA_AR$ clusters are present on neurons overexpressing Arf6 constructs. Primary hippocampal neurons were transfected with HA-tagged Arf6 wildtype, constitutively active (CA) mutant or dominant negative (DN) mutant and $GABA_AR$ clustering assessed by α2 subunit immunolabeling. B, Quantification of total eGFP-gephyrin cluster densities in cells co-expressing Arf6 constructs or expressing eGFP-gephyrin alone. Primary hippocampal cultures were transfected at DIV 8 and cells analyzed at DIV 15. Co-expression of Arf6 constructs had no effect on eGFP-gephyrin cluster density. C, Representative images and quantifications of eGFP-gephyrin apposition to VGAT. Cells co-expressing HA-Arf6 DN displayed a higher density of VGAT-non-apposed clusters and a lower percentage of VGAT-apposed clusters than cells co-expressing HA-Arf6 CA. Arrowheads indicate eGFP-gephyrin clusters not apposed to VGAT. D, Representative images and quantifications of eGFP-gephyrin apposition to VGluT1+2. Cells co-expressing HA-Arf6 DN displayed a higher density and percentage of eGFP-gephyrin clusters apposed to VGluT1+2 than cells co-expressing HA-Arf6 CA. Arrows indicate eGFP-gephyrin clusters apposed to VGluT1+2. Data points represent individual cells. **p<0.01, ***p<0.001; (see Table 1 for results of statistical analyses).

Figure 8

Analysis of IQSEC3 multimerization and neuronal somatic aggregation. A, Capacity of IQSEC3 constructs to multimerize was assessed by co-IP of mCherry-tagged IQSEC3 with corresponding FLAG-tagged IQSEC3 variants. mCherry-tagged and FLAG-tagged IQSEC3 constructs were co-expressed in HEK293T cells, lysates were immunoprecipitated with anti-FLAG antibody and co-immunoprecipitation of mCherry-tagged constructs was assessed by immunoblotting with anti-mCherry antibody. As negative controls, only mCherry tagged IQSEC3 was expressed (lane 1) and FLAG antibody was replaced by unspecific mouse IgG but both constructs were expressed (lane 2). Ratio of mCherry to FLAG immunoreactivity in immunoprecipitate was quantified. In all constructs mCherry-tagged variants were co-immunoprecipitated with FLAG-tagged variants. The mCherry to FLAG immunoprecipitate ratio was larger for IQSEC3 S348A than for wildtype IQSEC3. B, Analysis of somatic

aggregation of IQSEC3 in primary hippocampal neurons. Representative images and quantifications of somatic aggregates of FLAG-tagged IQSEC3 constructs are shown. Neuronal somata were blindly divided into cells containing small aggregates, large aggregates or both. Most cells overexpressing wildtype IQSEC3 contain small or large aggregates. Deletion of CC-domain containing N-terminus or mutation of IQ motif results in diffuse somatic distribution of IQSEC3 in most transfected cells. Small aggregates remain in IQSEC3 ΔN and large aggregates remain in IQ mutant. Overexpression of individual IQSEC3 domains is not sufficient for formation of somatic aggregates. *$p<0.05$; (see Table 3 for results of statistical analyses).

Tables

Table 1 Results of statistical tests performed on cluster density values

Figure	Conditions	One-way ANOVA	Bonferroni's multiple comparison test
3B	VGAT-apposed	F=0.406, p=0.749	-
	VGAT-non-apposed	F=28.295, p<0.001	Empty vector vs IQSEC3, t=1.468 Empty vector vs Sec7 mut., t=7.363 Empty vector vs IQ mut., t=0.222
	Percent VGAT-apposed	F=14.635, p<0.001	Empty vector vs IQSEC3, t=1.447 Empty vector vs Sec7 mut., t=5.022 Empty vector vs IQ mut., t=0.496
3C	VGluT1+2-apposed	F=15.525, p<0.001	Empty vector vs IQSEC3, t=0.944 Empty vector vs Sec7 mut., t=5.662 Empty vector vs IQ mut., t=0.741
	VGluT1+2-non-apposed	F=0.447, p=0.720	-
	Percent VGluT1+2-apposed	F=16.203, p<0.001	Empty vector vs IQSEC3, t=0.931 Empty vector vs Sec7 mut., t=5.815 Empty vector vs IQ mut., t=1.217
3D	Total cluster density	F=12.461, p<0.001	Empty vector vs IQSEC3, t=1.305 Empty vector vs Sec7 mut., t=4.748 Empty vector vs IQ mut., t=0.043
4B	VGAT-apposed	F=2.281, p=0.084	-
	VGAT-non-apposed	F=2.498, p=0.064	-
	Percent VGAT-apposed	F=1.604, p=0.193	-
4C	VGluT1+2-apposed	F=2.597, p=0.056	-
	VGluT1+2-non-apposed	F=0.486, p=0.693	-
	Percent VGluT1+2-apposed	F=1.165, p=0.327	-
4D	Total cluster density	F=2.775, p=0.042	Empty vector vs IQSEC3, t=0.094 Empty vector vs Sec7 mut., t=0.541 Empty vector vs IQ mut., t=2.579
5A	VGAT density	F=0.678, p=0.566	-
	VGAT-apposed to eGFP-gephyrin	F=0.378, p=0.769	-
5B	VGluT1+2 density	F=2.282, p=0.080	-
	VGluT1+2-apposed to eGFP-gephyrin	F=12.803, p<0.001	Empty vector vs IQSEC3, t=0.079 Empty vector vs Sec7 mut., t=5.597 Empty vector vs IQ mut., t=1.008
6B	VGAT-apposed	F=1.674, p=0.181	-
	VGAT-non-apposed	F=7.558, p<0.001	Neighb. untr. vs IQSEC3, t=0.106 Neighb. untr. vs Sec7 mut., t=3.698 IQSEC3 vs Sec7 mut., t=3.888
	Percent VGAT-apposed	F=7.164, p<0.001	Neighb. untr. vs IQSEC3, t=0.130 Neighb. untr. vs Sec7 mut., t=4.146 IQSEC3 vs Sec7 mut., t=3.314
6D	VGluT1+2-apposed	F=5.117, p=0.005	Neighb. untr. vs IQSEC3, t=0.935 Neighb. untr. vs Sec7 mut., t=3.148 IQSEC3 vs Sec7 mut., t=2.569
	VGluT1+2-non-apposed	F=1.057, p=0.379	-
	Percent VGluT1+2-apposed	F=8.243, p<0.001	Neighb. untr. vs IQSEC3, t=0.961 Neighb. untr. vs Sec7 mut., t=3.862 IQSEC3 vs Sec7 mut., t=3.501
7B	Total cluster density	F=2.543, p=0.059	-
7C	VGAT-apposed	F=1.779, p=0.159	-
	VGAT-non-apposed	F=4.159, p=0.009	Untr. vs Arf6 CA, t=1.105 Untr. vs Arf6 DN, t=2.452 Arf6 CA vs Arf6 DN, t=3.371
	Percent VGAT-apposed	F=6.523, p<0.001	Untr. vs Arf6 CA, t=1.088 Untr. vs Arf6 DN, t=3.284 Arf6 CA vs Arf6 DN, t=4.119
7D	VGluT1+2-apposed	F=6.625, p<0.001	Untr. vs Arf6 CA, t=0.283 Untr. vs Arf6 DN, t=3.382 Arf6 CA vs Arf6 DN, t=4.115
	VGluT1+2-non-apposed	F=0.809, p=0.493	-

	Percent VGluT1+2-apposed	F=6.106, p<0.001	Untr. vs Arf6 CA, t=0.979 Untr. vs Arf6 DN, t=2.866 Arf6 CA vs Arf6 DN, t=3.808

F and t represent test statistics for one-way ANOVA and Bonferroni's multiple comparison tests, respectively.

Table 2 Results of statistical tests performed on cluster size values

Figure	Conditions	Kruskal-Wallis test	Dunn's multiple comparison test
3E	eGFP-gephyrin cluster size	n=7027, H=30.161, p<0.001	E. v. vs IQSEC3, y=213.368, p<0.01 E. v. vs Sec7 mut., y=317.373, p<0.001 E. v. vs IQ mut., y=316.009, p<0.001
4E	GFP-PSD-95 cluster size	n=9707, H=2.866, p=0.413	-

H and y represent test statistics for Kruskal-Wallis test and Dunn's multiple comparison test, respectively.

Table 3 Results of statistical tests used for co-IP quantification

Figure	One-way ANOVA	Conditions	Dunnett's multiple comparison test
8A	F=3.253, p=0.020	Wildtype vs IQSEC3 ΔN	P=0.778
		Wildtype vs IQ mutant	P=0.998
		Wildtype vs IQSEC3 S348A	P=0.021
		Wildtype vs IQSEC3 S348E	P=0.989
		Wildtype vs IQSEC3 S348R	P=0.995
		Wildtype vs Sec7 mutant	P=0.992

F represents test statistic for one-way ANOVA.

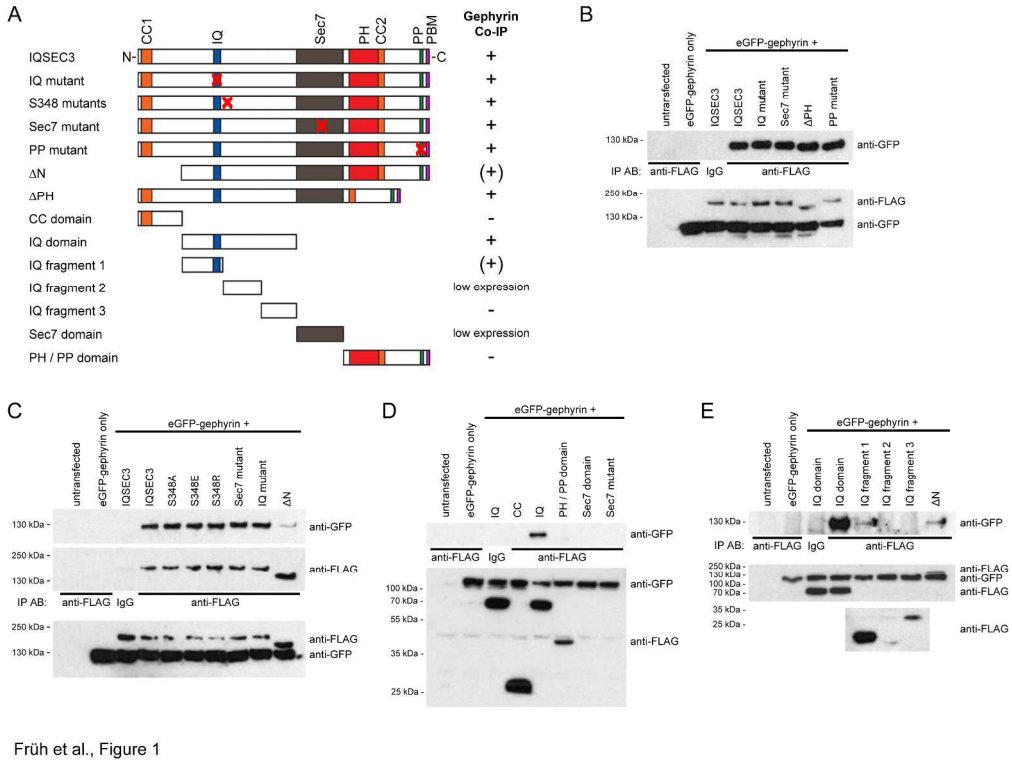

Figure 1:
IQSEC3 interacts with gephyrin G- or C-domain near the IQ motif. A, Schematic overview of IQSEC3 constructs and summary of gephyrin interaction results. Binding to gephyrin is indicated by "+", "(+)" indicates weaker binding compared to wildtype IQSEC3 and "-" indicates absence of binding. B-E, Representative Western blots of co-immunoprecipitation (co-IP) experiments performed to assess IQSEC3 interaction with gephyrin. In all experiments, constructs were expressed in HEK293T cells and lysates used for co-IP using mouse anti-FLAG antibody bound to agarose beads. Two negative controls were employed to exclude unspecific binding. Anti-FLAG antibody was replaced by unspecific mouse IgG but both constructs were expressed. In addition, the construct to be immunoprecipitated was not expressed but immunoprecipitation antibody was present. B, Mutation of IQ motif, Sec7 catalytic domain and PP motif, as well as deletion of PH domain, do not hinder binding of IQSEC3 to gephyrin. C, Mutation of IQSEC3 S348 does not affect binding to gephyrin but N-terminal CC domain is necessary for efficient interaction with gephyrin. D, IQ domain is sufficient for gephyrin binding and CC domain, which is missing in N-terminal deletion, itself does not bind gephyrin. For constructs encoding Sec7 domain and Sec7 domain containing E749K mutation (Sec7 mutant) expression in HEK293T cells was too week to assess interaction by co-IP. E, Gephyrin binds to a region near the IQ motif in IQSEC3. IQ fragment 1 was detected in immunoprecipitates but not IQ fragment 3. Expression of IQ fragment 2 in HEK293T cells was too weak to assess binding to gephyrin.

251x190mm (300 x 300 DPI)

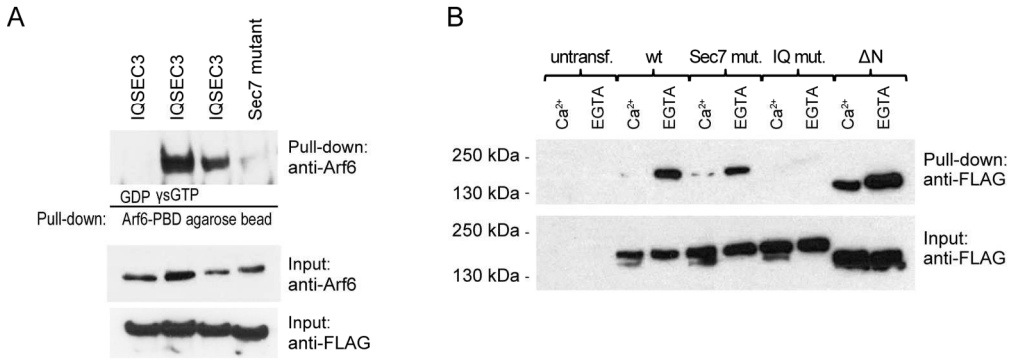

Früh et al., Figure 2

Figure 2:
Validation of functional significance of IQSEC3 mutations. A, Arf6 activation assay demonstrating that E749K mutation abolishes activation of Arf6 by IQSEC3. The upper blot depicts Arf6 immunoreactivity following pull-down of activated Arf6. The lower blot is the loading control. B, Apocalmodulin binds to IQSEC3 IQ motif. Representative Western blot of calmodulin pull-down of IQSEC3 constructs in high and low Ca2+ conditions. IQSEC3 binds to calmodulin more efficiently in low Ca2+ conditions and requires IQ motif for interaction. IQSEC3 constructs were overexpressed in HEK293T cells and lysates used for calmodulin pull-down assay in the presence of 2 mM CaCl2 or 2 mM EGTA.

155x78mm (300 x 300 DPI)

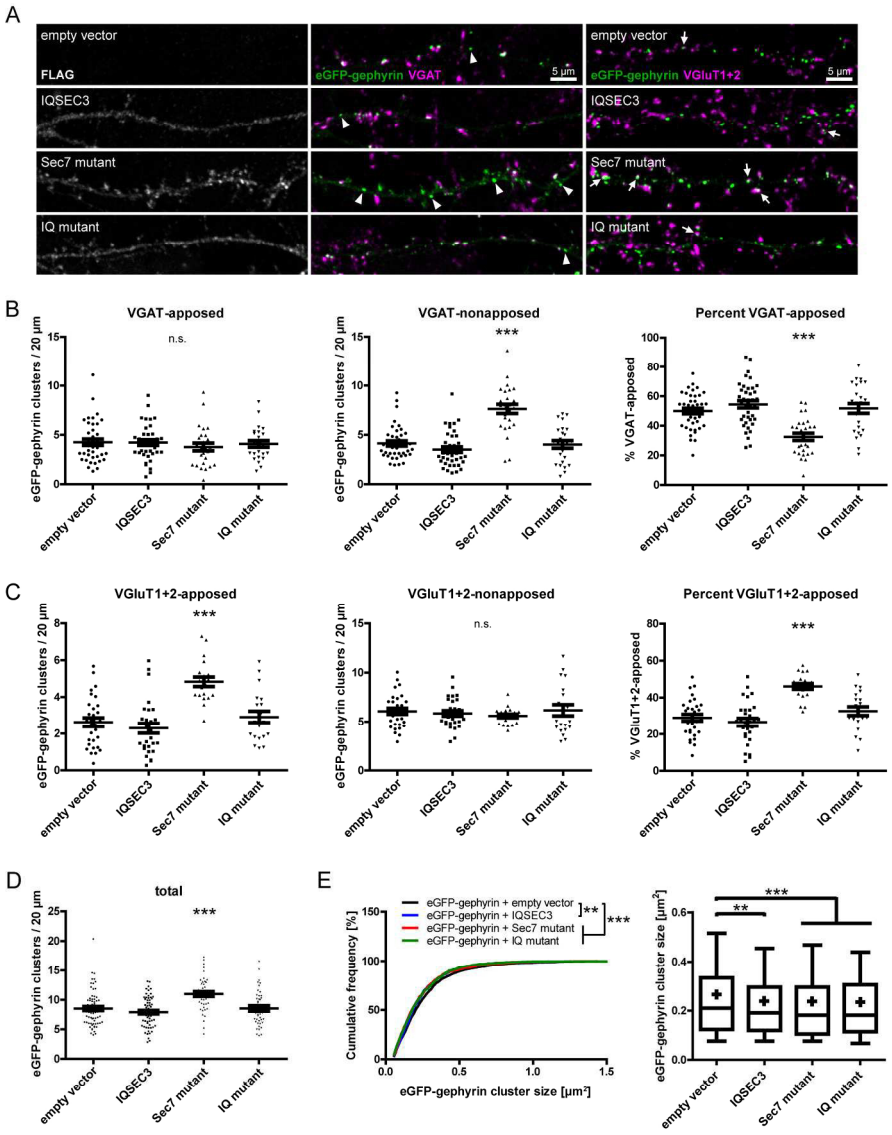

Früh et al., Figure 3

Figure 3:

The catalytic function of IQSEC3 regulates apposition of gephyrin to presynaptic terminals. FLAG-tagged IQSEC3 constructs or an empty vector were co-expressed with eGFP-gephyrin in primary hippocampal neurons at DIV 8 and apposition to VGAT or VGluT1+2 immunofluorescent puncta assessed at DIV 15. A, Representative images of dendrites of transfected cells. FLAG immunoreactivity is shown in cells co-labeled for VGAT. IQSEC3 Sec7 mutant-overexpressing cells exhibit an increased amount of VGAT-non-apposed eGFP-gephyrin clusters (arrowheads) in comparison to all other constructs. VGluT1+2-apposed eGFP-gephyrin clusters (arrows) are also more abundant in cells overexpressing Sec7 mutant. B, Quantification of eGFP-gephyrin VGAT apposition. VGAT-apposed eGFP-gephyrin cluster density was not significantly different between constructs. In contrast, VGAT-non-apposed eGFP-gephyrin clusters displayed an increased density in Sec7 mutant-expressing cells compared to all other constructs, resulting in a decreased percentage of VGAT-apposed eGFP-gephyrin clusters. C, Quantification of eGFP-gephyrin VGluT1+2 apposition. VGluT1+2-apposed eGFP-gephyrin cluster density was increased by overexpression of Sec7 mutant but in VGluT1+2-

non-apposed eGFP-gephyrin clusters no significant differences were found between groups. The increase of VGluT1+2-apposed eGFP-gephyrin cluster density in Sec7 mutant-expressing neurons is reflected in a higher percentage of VGluT1+2-apposed eGFP-gephyrin clusters. D, Quantification of total dendritic eGFP-gephyrin cluster densities. Overexpression of IQSEC3 Sec7 mutant led to an increase in eGFP-gephyrin cluster density whereas IQSEC3 wildtype or IQ mutant did not significantly change eGFP-gephyrin cluster density. E, Quantification of overall eGFP-gephyrin cluster size in cells co-expressing IQSEC3 constructs. Compared to empty vector, all IQSEC3 constructs caused a small but statistically significant reduction of cluster size when co-expressed with eGFP-gephyrin. In box plots, lines, crosses, boxes and whiskers represent median, mean, 25-75 percentile and 10-90 percentile, respectively. Data points represent individual cells. **p<0.01, ***p<0.001; (see Tables 1-2 for results of statistical analyses).

179x243mm (300 x 300 DPI)

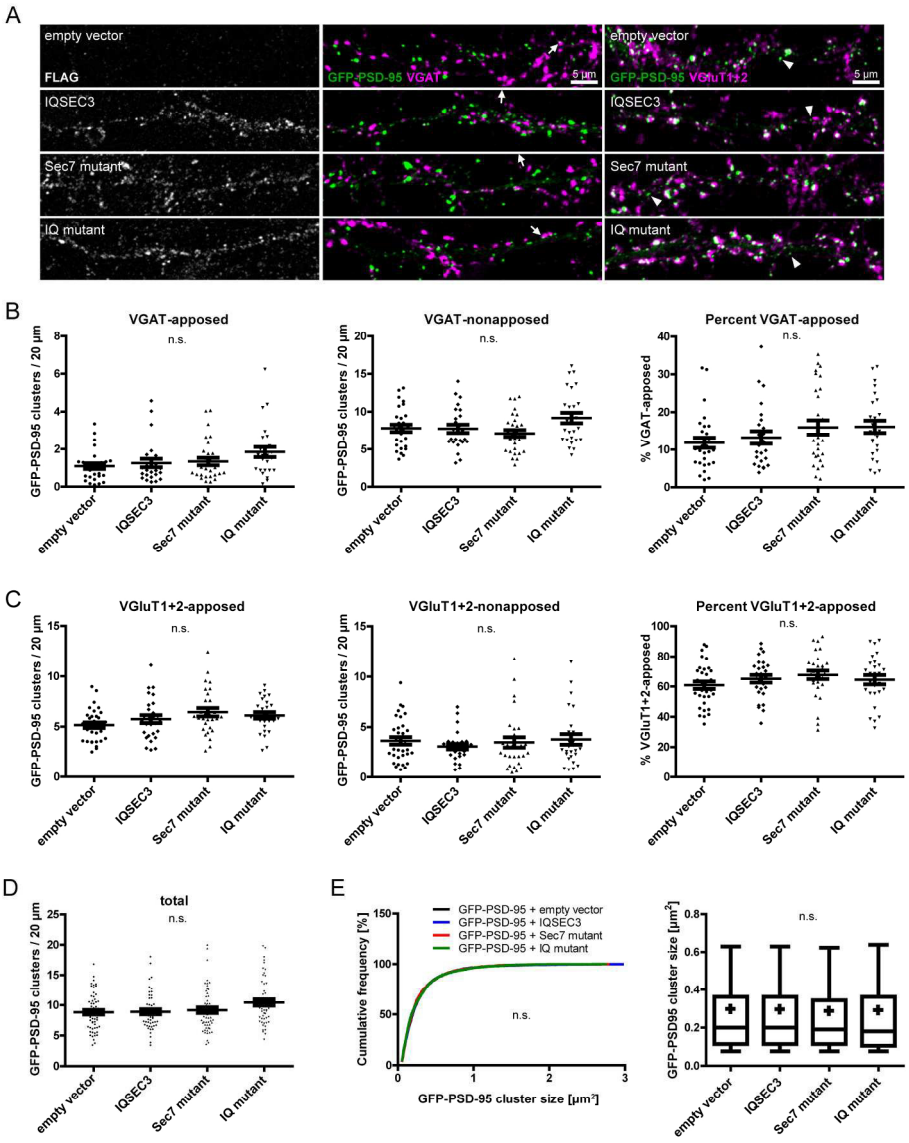

Früh et al., Figure 4

Figure 4:
IQSEC3 catalytic function is not involved in regulation of presynaptic apposition of glutamatergic postsynaptic density. FLAG-tagged IQSEC3 constructs were co-expressed with GFP-PSD-95 in primary hippocampal neurons at DIV 8 and apposition to presynaptic markers analyzed at DIV 15. A, Representative images of dendrites of transfected cells immunolabeled either for VGAT or VGluT1+2. FLAG immunoreactivity is shown in cells co-labeled for VGAT. The majority of GFP-PSD-95 clusters is apposed to VGluT1+2 puncta but a minor fraction of clusters is mis-apposed to VGAT (arrows) or is not apposed to VGluT1+2 (arrowheads). B-E, Quantification of clustering and apposition parameters of GFP-PSD-95. In all analyses, there were no statistically significant differences found between constructs. B, Quantification of VGAT apposition of GFP-PSD-95. C, Quantification of VGluT1+2 apposition of GFP-PSD-95. D, Quantification of total dendritic GFP-PSD-95 cluster densities. E, Quantification of overall GFP-PSD-95 cluster size. In box plots, lines, crosses, boxes and whiskers represent median, mean, 25-75 percentile and 10-90 percentile, respectively. Data points represent individual cells; (see Tables 1-2 for results of statistical analyses).

176x235mm (300 x 300 DPI)

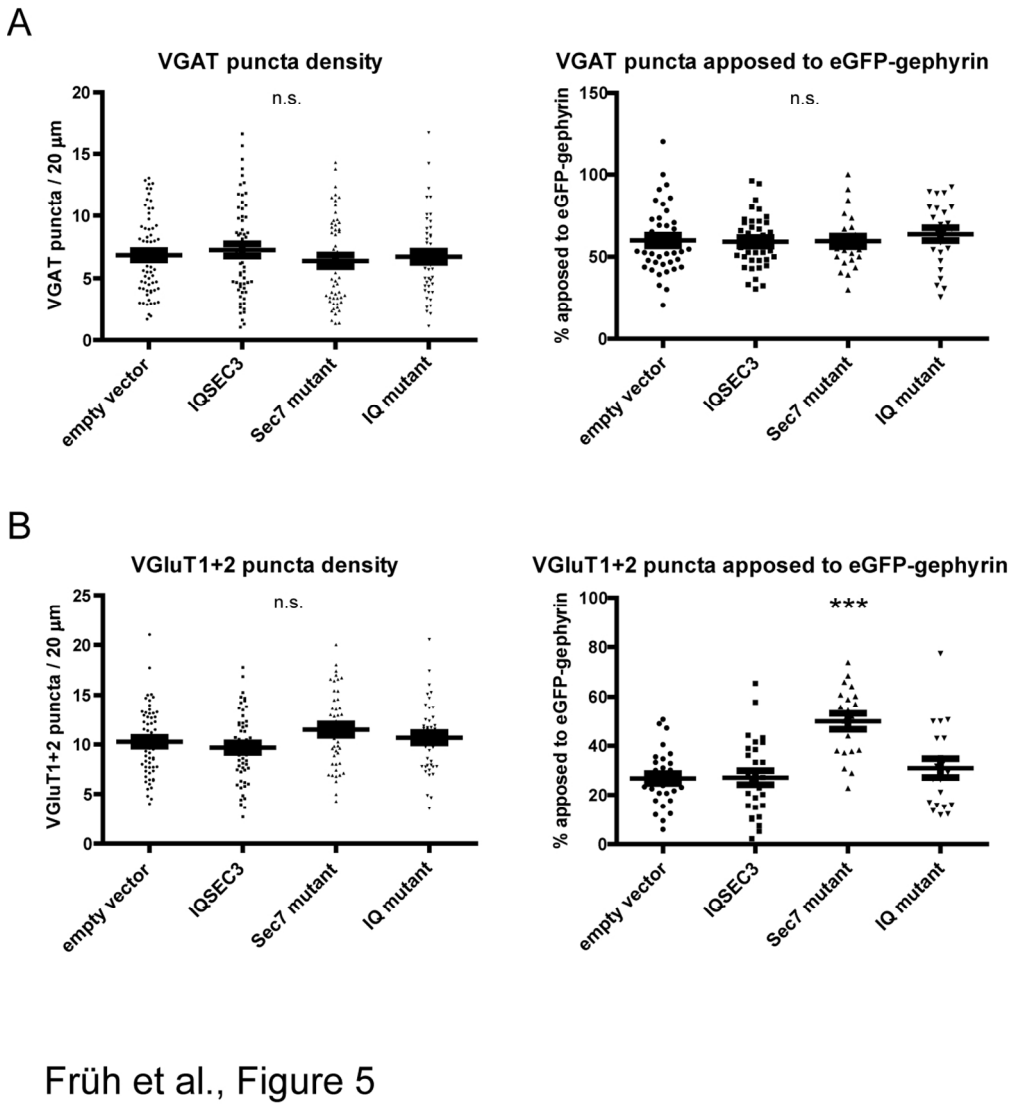

Früh et al., Figure 5

Figure 5:
Fraction of mismatched glutamatergic presynaptic terminals but not innervation density is affected by IQSEC3 catalytic function. A, Quantification of VGAT puncta densities and percentage of VGAT puncta apposed to eGFP-gephyrin. Co-expression of IQSEC3 constructs had no statistically significant effect on puncta density or percentage of apposition to eGFP-gephyrin. B, Quantification of VGluT1+2 puncta densities and percentage of VGluT1+2 puncta apposed to eGFP-gephyrin. Percentage of VGluT1+2 puncta apposed to eGFP-gephyrin was increased in Sec7 mutant-overexpressing cells compared to all other groups but absolute VGluT1+2 densities were unaffected by IQSEC3 construct co-expression. Data points represent individual cells. ***p<0.001; (see Table 1 for results of statistical analyses).

111x122mm (300 x 300 DPI)

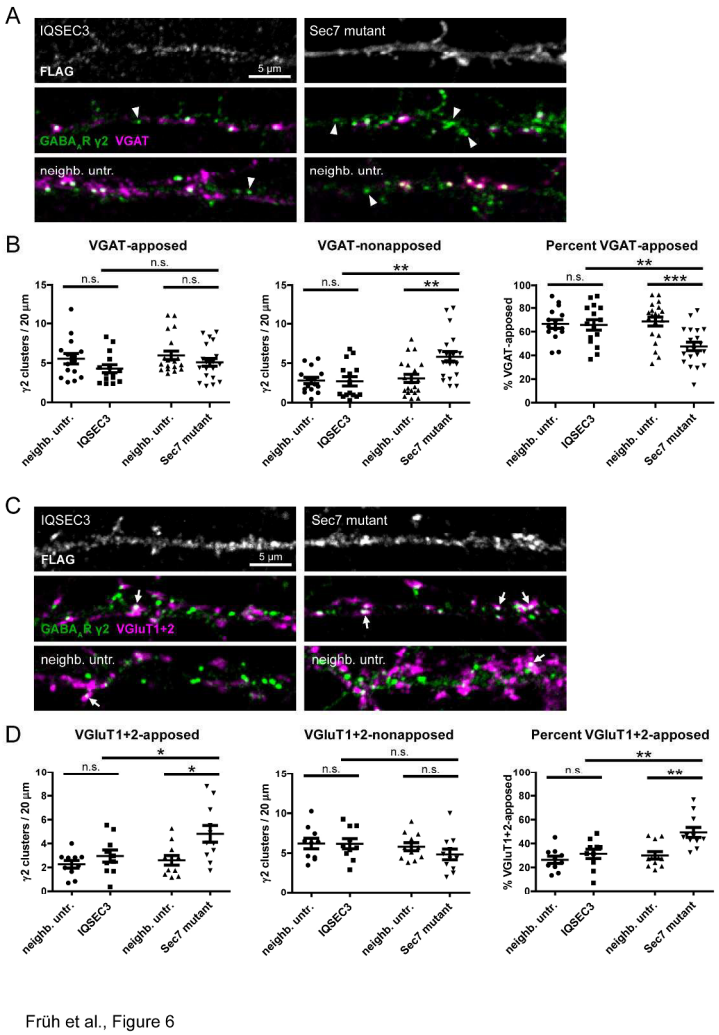

Früh et al., Figure 6

Presynaptic apposition of GABAA receptors is regulated by IQSEC3 catalytic function. Primary hippocampal neurons were transfected with IQSEC3 wildtype or Sec7 mutant constructs at DIV 8 and presynaptic apposition of GABAAR γ2 subunit clusters analyzed at DIV 15. Untransfected dendrites neighboring transfected cells served as control. A, Representative images of dendrites of cells transfected with IQSEC3 constructs (upper panels; FLAG immunolabeling shown) and untransfected neighboring dendrites (lower panels) immunolabeled for VGAT. Note the high abundance of GABAAR γ2 subunit clusters not apposed to VGAT (arrowheads) in dendrites of cells transfected with Sec7 mutant. B, Quantification of GABAAR γ2 subunit cluster VGAT apposition. Compared to untransfected neighboring dendrites and to cells overexpressing wildtype IQSEC3, cells overexpressing Sec7 mutant show elevated VGAT-non-apposed cluster densities, reflected in a lower percentage of VGAT-apposed clusters. C, Representative images of dendrites of cells transfected with IQSEC3 constructs (upper panels; FLAG immunolabeling shown) and untransfected neighboring dendrites (lower panels) immunolabeled for VGluT1+2. Note the high abundance of GABAAR γ2 subunit clusters apposed to VGluT1+2 puncta (arrows) in dendrites of cells overexpressing

Sec7 mutant. D, Quantification of GABAAR γ2 subunit cluster VGluT1+2 apposition. Sec7 mutant-transfected cells showed significantly higher density of VGluT1+2-apposed GABAAR γ2 subunit clusters compared to untransfected cells and to cells transfected with wildtype IQSEC3. The increase in VGluT1+2-apposed cluster density is mirrored by a higher percentage of VGluT1+2-apposed clusters. Data points represent individual cells. *p<0.05, **p<0.01, ***p<0.001; (see Table 1 for results of statistical analyses).

210x297mm (300 x 300 DPI)

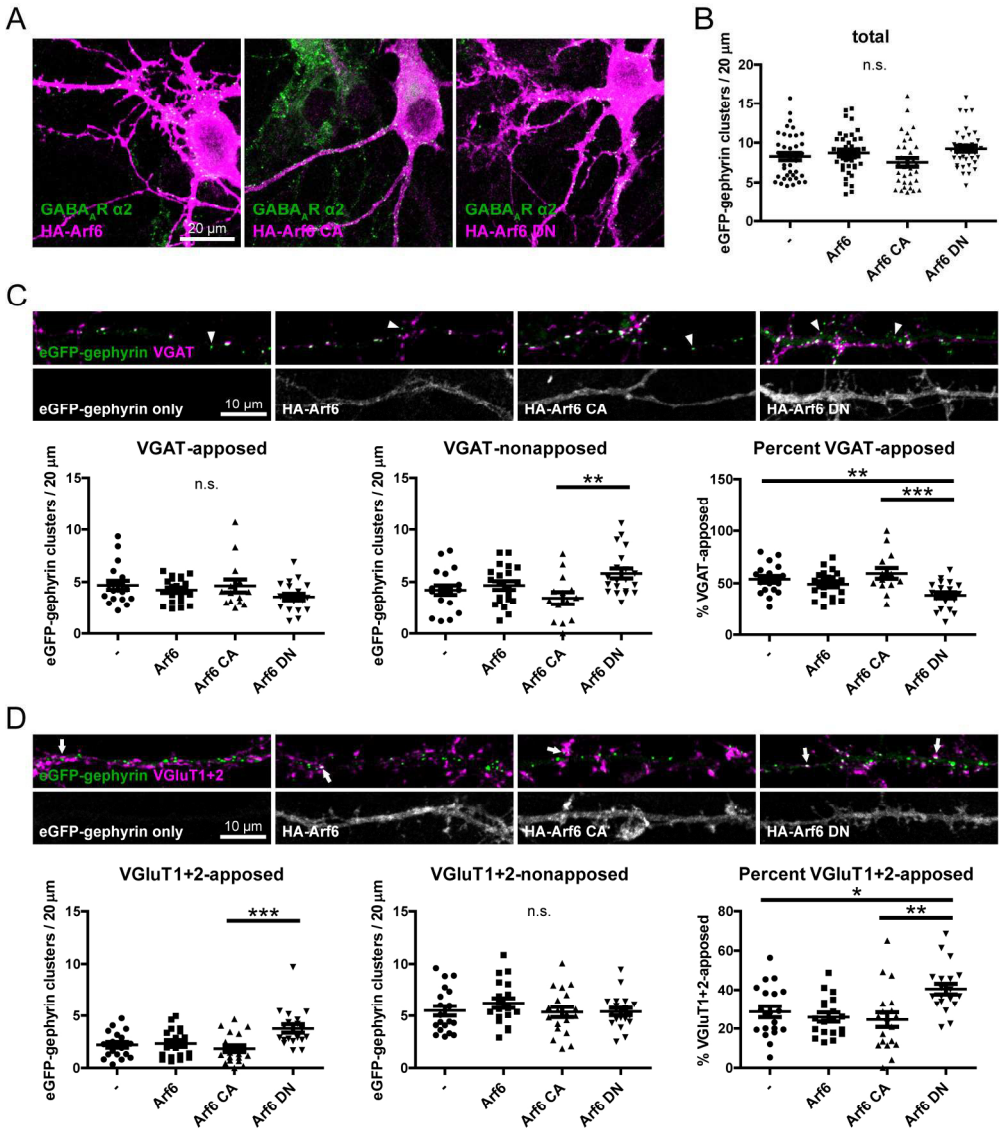

Früh et al., Figure 7

Figure 7:

Arf6 is involved in regulation of gephyrin presynaptic apposition. A, GABAAR clusters are present on neurons overexpressing Arf6 constructs. Primary hippocampal neurons were transfected with HA-tagged Arf6 wildtype, constitutively active (CA) mutant or dominant negative (DN) mutant and GABAAR clustering assessed by α2 subunit immunolabeling. B, Quantification of total eGFP-gephyrin cluster densities in cells co-expressing Arf6 constructs or expressing eGFP-gephyrin alone. Primary hippocampal cultures were transfected at DIV 8 and cells analyzed at DIV 15. Co-expression of Arf6 constructs had no effect on eGFP-gephyrin cluster density. C, Representative images and quantifications of eGFP-gephyrin apposition to VGAT. Cells co-expressing HA-Arf6 DN displayed a higher density of VGAT-non-apposed clusters and a lower percentage of VGAT-apposed clusters than cells co-expressing HA-Arf6 CA. Arrowheads indicate eGFP-gephyrin clusters not apposed to VGAT. D, Representative images and quantifications of eGFP-gephyrin apposition to VGluT1+2. Cells co-expressing HA-Arf6 DN displayed a higher density and percentage of eGFP-gephyrin clusters apposed to VGluT1+2 than cells co-expressing HA-Arf6 CA. Arrows indicate eGFP-gephyrin

clusters apposed to VGluT1+2. Data points represent individual cells. **p<0.01, ***p<0.001; (see Table 1 for results of statistical analyses).

180x217mm (300 x 300 DPI)

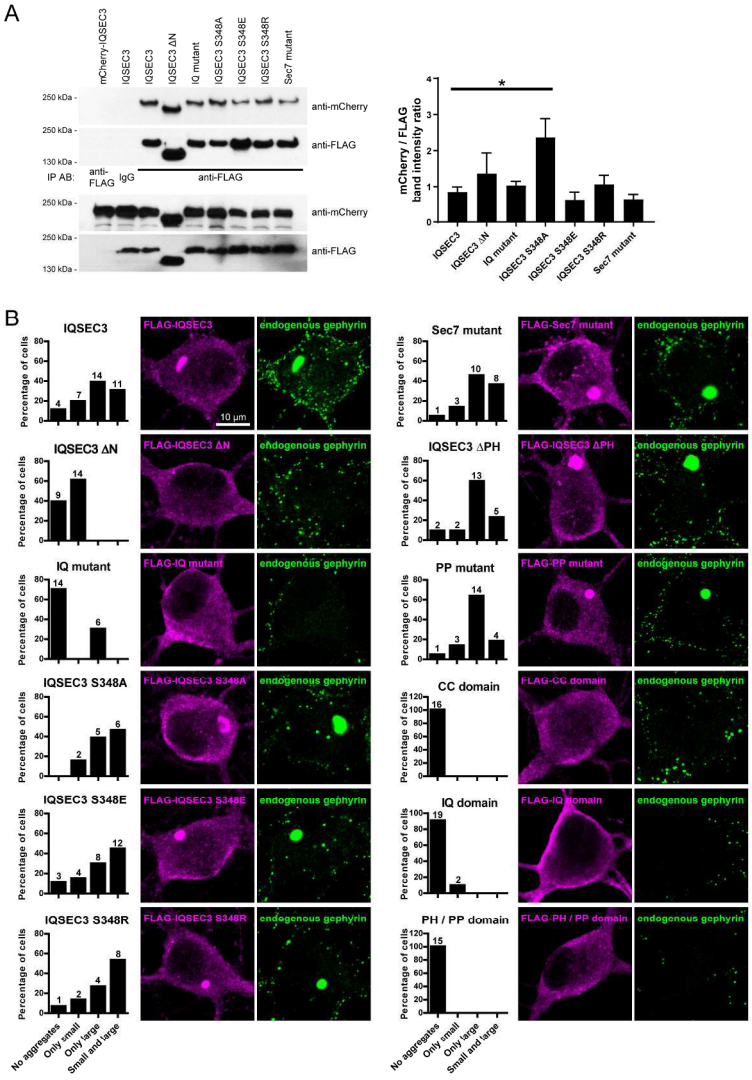

Früh et al., Figure 8

Analysis of IQSEC3 multimerization and neuronal somatic aggregation. A, Capacity of IQSEC3 constructs to multimerize was assessed by co-IP of mCherry-tagged IQSEC3 with corresponding FLAG-tagged IQSEC3 variants. mCherry-tagged and FLAG-tagged IQSEC3 constructs were co-expressed in HEK293T cells, lysates were immunoprecipitated with anti-FLAG antibody and co-immunoprecipitation of mCherry-tagged constructs was assessed by immunoblotting with anti-mCherry antibody. As negative controls, only mCherry tagged IQSEC3 was expressed (lane 1) and FLAG antibody was replaced by unspecific mouse IgG but both constructs were expressed (lane 2). Ratio of mCherry to FLAG immunoreactivity in immunoprecipitate was quantified. In all constructs mCherry-tagged variants were co-immunoprecipitated with FLAG-tagged variants. The mCherry to FLAG immunoprecipitate ratio was larger for IQSEC3 S348A than for wildtype IQSEC3. B, Analysis of somatic aggregation of IQSEC3 in primary hippocampal neurons. Representative images and quantifications of somatic aggregates of FLAG-tagged IQSEC3 constructs are shown. Neuronal somata were blindly divided into cells containing small aggregates, large aggregates or both. Most cells overexpressing wildtype IQSEC3 contain small or large aggregates. Deletion of CC-domain containing N-

terminus or mutation of IQ motif results in diffuse somatic distribution of IQSEC3 in most transfected cells. Small aggregates remain in IQSEC3 ΔN and large aggregates remain in IQ mutant. Overexpression of individual IQSEC3 domains is not sufficient for formation of somatic aggregates. *p<0.05; (see Table 3 for results of statistical analyses).

210x297mm (300 x 300 DPI)

JNC-2018-0034

The catalytic function of the gephyrin-binding protein IQSEC3 regulates…

Früh et al.

“In this issue”:

During synapse formation, proteins of the postsynaptic density are properly sorted and aggregated at sites facing the presynaptic terminal releasing a specific neurotransmitter, e.g. GABA versus glutamate. This study reports that the guanine nucleotide exchange factor IQSEC3, activating the small GTPase of the ADP-ribosylation factor family Arf6, regulates the proper matching of the postsynaptic protein gephyrin in GABAergic versus glutamatergic synapses. IQSEC3 function is modulated by binding to gephyrin and calmodulin and activation of Arf6 by IQSEC3 selectively reduces postsynaptic clustering of gephyrin in glutamatergic synapses.

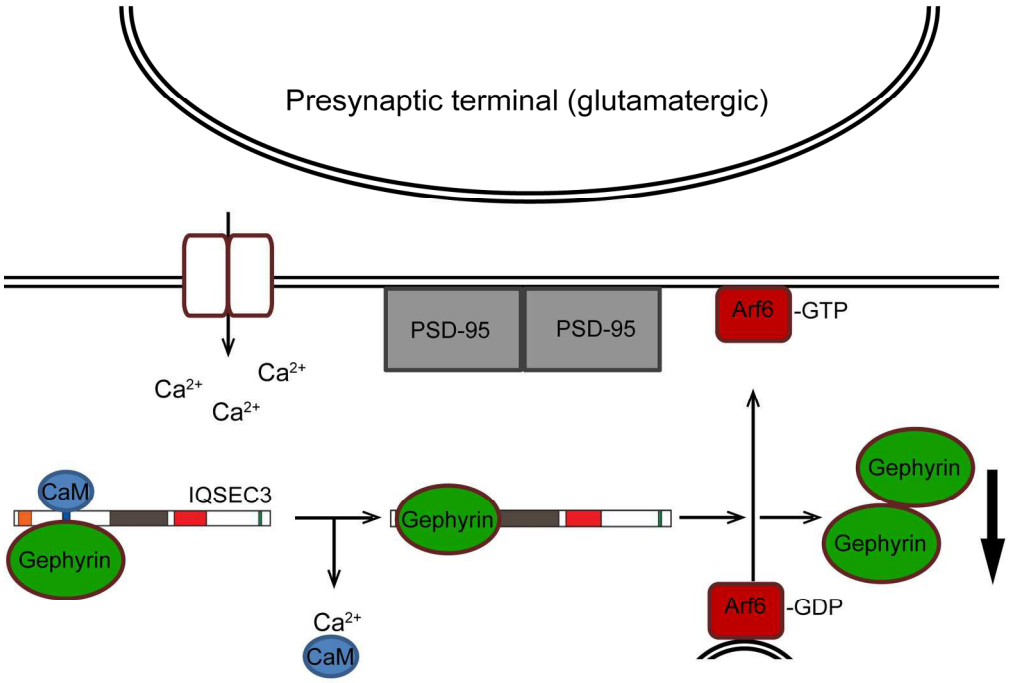

169x170mm (300 x 300 DPI)